CASE FILE
COPY

NASA CONTRACTOR
REPORT

65N15745

NASA CR-157

NASA CR-157

A DESCRIPTION OF A COMPUTER PROGRAM FOR THE STUDY OF ATMOSPHERIC EFFECTS ON SONIC BOOMS

by Manfred P. Friedman

Prepared under Contract No. NAS 1-2511 *by*
MASSACHUSETTS INSTITUTE OF TECHNOLOGY
Cambridge, Mass.
for

NATIONAL AERONAUTICS AND SPACE ADMINISTRATION • WASHINGTON, D. C. • FEBRUARY 1965

NASA CR-157

A DESCRIPTION OF A COMPUTER PROGRAM FOR THE STUDY OF ATMOSPHERIC EFFECTS ON SONIC BOOMS

By Manfred P. Friedman

Distribution of this report is provided in the interest of information exchange. Responsibility for the contents resides in the author or organization that prepared it.

Prepared under Contract No. NAS 1-2511 by
MASSACHUSETTS INSTITUTE OF TECHNOLOGY
Cambridge, Mass.

for

NATIONAL AERONAUTICS AND SPACE ADMINISTRATION

For sale by the Office of Technical Services, Department of Commerce,
Washington, D.C. 20230 -- Price $3.00

FOREWORD

The work done on this project was supported by NASA, Contract NAS 1-2511. Some of the computer work was done at the Computation Center at MIT, Cambridge, Massachusetts.

The author wishes to thank Mr. Charles Bartlett of MIT for his many helpful suggestions.

ABSTRACT

An approach to the problem of a shock propagating through a variable atmosphere is presented. A previously presented theory has been improved and a computer program has been written using the results of the improved theory. This paper presents the improved results and gives a detailed description of the computer program.

For an atmosphere which varies arbitrarily in the vertical direction and for a supersonic aircraft with arbitrary lift and volume distribution the computer program will give the shock overpressure and intersection points at the ground. In addition, effects due to aircraft acceleration, flight path angle and curvature and acoustical cutoff are computed and presented by the program.

TABLE OF CONTENTS

Section		Page
	FOREWORD	iii
	ABSTRACT	v
I.	INTRODUCTION	1
II.	PROGRAM OPERATION DETAILS	3
	II.1 INPUT FORMAT	3
	II.2 OUTPUT FORMAT	7
	II.3 PROGRAM LIMITATIONS	7
III.	PROGRAM DETAILS	9
	III.1 EQUATIONS	9
	III.2 PROGRAM SYMBOLS (FORTRAN)	17
	III.3 SUBROUTINES	19
IV.	IMPROVEMENTS TO THE THEORY	23
	IV.1 THE PRESSURE JUMP EXPRESSION	23
	IV.2 RAY TUBE AREA	25
Appendices		
I.	REFERENCES	27
II.	TWO SAMPLE PROBLEMS	29
III.	FORTRAN LISTING	35
IV.	CLIMBING, DIVING, AND FLIGHT PATH CURVATURE EFFECTS	47
	AIV.1 RAY ANGLE GEOMETRY	47
	AIV.2 FLIGHT PATH CURVATURE	50
	AIV.3 SHOCK GROUND INTERSECTION	54
	AIV.4 PROGRAM DETAILS	55
V.	EXPERIMENTAL RESULTS	57

SECTION I

INTRODUCTION

This report will give a description of a "Sonic Boom Computer Program".* The theoretical development, upon which the computer program is based, is presented in Section IV and Ref. 1. Since the emphasis here is for the operation of the SBCP, discussion of the theoretical results will be kept to a minimum.

The SBCP uses the following input data:

1) Atmospheric pressure, temperature and winds between the aircraft and the ground, and shock-ground reflection factor.

2) Aircraft parameters such as Mach number, altitude, acceleration rate, volume and lift factors, aircraft length and weight.

3) The analysis is based on ray tube concepts, that is, a small segment of shock is considered to be propagating down a ray tube and its strength and location are determined along the ray path until it strikes the ground. Therefore, another input is the initial ray directions. These are specified by giving those angles, measured around the flight direction, for which computations are desired. (That is, the angles Φ in Fig. 1, Section II).

The computer output gives:

1) A listing of pertinent input data.

2) The location and strength of the shock corresponding to a selected input angle at intermediate computed points between the aircraft and the ground.

3) The location and strength of the shock at the shock-ground intersection.

The program was written in Fortran II and has been operated on IBM 709, 7090 and 7094 computers.

---

* In the remainder of this report the "Sonic Boom Computer Program" will be denoted by SBCP.

Details for operating the program are given in Section II. The equations which are actually solved are presented in Section III. In addition the Fortran symbols and their corresponding physical variables and a brief descriptions of the subroutines are given in this section. Some improvements to the theory are given in Section IV. In Appendix II the input and output for two sample problems are given. A listing of the Fortran program deck is given in Appendix III. In Appendix IV the theory is extended to include aircraft diving or climbing and curved flight path effects. Results of some sample computations are given in Appendix V.

SECTION II

PROGRAM OPERATION DETAILS

II.1 INPUT FORMAT

In order to operate the program the data cards must be arranged in the following manner:

Control card: The first card is a control card, it tells the following:

1) The number of altitudes at which atmospheric data will be prescribed, this number can be 2 to 100. That is a minimum of 2 altitudes (aircraft and ground) are required to run any problem and a maximum of 100 altitudes can be handled. This number should be entered so that the last digit is in column 10.

2) The number of angles, measured about the aircraft axis, for which output data is desired (see "angle cards", p.4). A minimum of 1 and a maximum of 21 different angles can be prescribed, therefore this number can be 1 to 21. It should be entered so that the last digit is in column 20.

3) A problem identification number. This can be any integer from 0 to 99999. It should be entered so that the last digit is in column 30.

4) The input angles mentioned in (2) above can be entered in any order. However it is necessary to know which of these angles corresponds to the direction directly below the aircraft. The next entry on the control card tells which of the input angles corresponds to this direction. This can therefore be a number between 1 and 21. It should be entered so that the last digit is in column 40.

5) Part of the output is a listing of the shock strength and location for one of the input angles at computed points between the aircraft and the ground. That is, a time history of the shock propagation is given. The next entry tells which one of the input angles this information should correspond to. This can therefore be a number between 1 and 21. It should be entered so that the last digit is in column 50.

6) The last entry on the control card tells the computer whether or not another problem (different atmosphere, different aircraft, etc.) follows the completion of the problem currently being entered. A negative number in columns 51 to 60 will stop the computer at the end of the current computation; no entry or a positive entry will have the computer read in a new set of data after completion of the current problem.

All the numbers entered on the control card are fixed point integers. That is, no decimal point should be used and the first five entries should appear in the columns indicated. The last entry (if any) can go anywhere between columns 51 and 60.

Atmosphere Cards: After the control card the next cards carry atmospheric data. There will be one card for each altitude at which atmospheric data is prescribed. (The number of atmosphere cards is equal to the first number entered on the control card.)

These cards are entered so that the highest altitude is first, then descending in altitude, and the lowest altitude (ground) last. Each card has the same format and tells the altitude and the pressure, temperature, headwind and sidewind corresponding to that altitude. All numbers must have their decimal point and can appear anywhere within the columns indicated below.

Columns	Data	
1 – 10	altitude ÷ 1000.	in feet
11 – 20	pressure	pounds/sq. ft.
21 – 30	temperature	deg. F
31 – 40	headwind	ft./sec.
41 – 50	sidewind	ft./sec.

The winds should be referenced to the aircraft direction. A headwind is positive and a tailwind is negative. A sidewind in the direction of the starboard wing is positive, in the direction of the port wing is negative.

Angle cards: The computation starts with an initial ray direction and determines shock properties all along this ray until it meets the ground. The initial ray directions are determined by the "angle input", these are angles measured about the aircraft ray (or shock) cone axis. The angle $\phi = 0$

corresponds to directly below the aircraft. In Fig II.1 the aircraft is moving in the direction of the negative x axis and is coming out of the paper toward the reader.

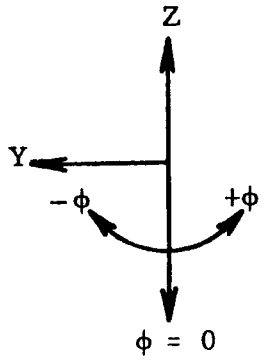

$\phi = 0$ corresponds to directly below the aircraft

Figure II. 1

As many as 21 different angles ϕ can be specified, they can be entered in any order and are measured in degrees. The numbers must have their decimal point and are entered 7 numbers per card as follows:

Columns	Data				
1 – 10	first	angle in degrees			
11 – 20	second	"	"	"	(if necessary)
61 – 70	seventh	"	"	"	"
1 – 10 next card	eighth	"	"	"	" , etc.

The angle (with decimal point) can appear anywhere within the indicated columns. The number of successive columns of ten needed for entering all the angles is equal to the second number entered on the control card.

One of the angles entered must be zero ($\phi = 0.0$). The number corresponding to the position of the angle $\phi = 0.0$ in the above array is the fourth entry on the control card. One of the angles can be selected to have a history of the shock properties between the aircraft and the ground printed out, the number corresponding to the position of this angle in the above array is the fifth entry on the control card.

Aircraft data cards: The last input cards give thirteen pieces of data by which the aircraft, flight conditions, and shock-ground reflection factor are specified. For each of these numbers there are ten columns on the input card, the numbers must be entered with their decimal point and can appear anywhere within the field of ten columns. The order of entry is as follows:

Columns		Data
1-10	first card	aircraft acceleration, ft/sec.^{2}
11-20	" "	aircraft length, ft.
21-30	" "	shock-ground reflection constant
31-40	" "	aircraft Mach number
41-50	" "	aircraft altitude, ft.
51-60	" "	aircraft volume factor
61-70	" "	aircraft lift factor
1-10	second card	aircraft weight, lb.
11-20	" "	aircraft fineness ratio (length/max. diameter)
21-30	" "	effective wing chord for lift distribution, ft.
31-40	" "	flight path curvature x 10^6, 1/ft.
41-50	" "	climb (or dive) angle, deg.
51-60	" "	time increment, sec.

The last three entries above involve aircraft dive and climb calculations, they are defined in Appendix IV. Details of the integration of body shape and lift distribution source terms are not carried out in the SBCP. An asymptotic "aircraft shape term" is used (See Section III.1, Eq. III.13). This term is given below:

Shock overpressure at the ground

$$\Delta P = P_g \times RC \times \left\{\begin{matrix}\text{atmospheric and}\\ \text{propagation terms}\end{matrix}\right\} \times \left\{\begin{matrix}\text{aircraft}\\ \text{shape terms}\end{matrix}\right\} \times \left\{\frac{4M^3}{M^2-1}\right\}^{1/4}$$

$$\begin{matrix}\text{aircraft}\\ \text{shape terms}\end{matrix} = \sqrt{\left(\frac{VF \cdot L^{.75}}{FR}\right)^2 + \cos\phi \cdot \frac{\sqrt{M^2-1} \cdot (LF)^2 \cdot WT}{M^2 \cdot P_h \cdot (WC)^{.5}}}$$

P_g = atmospheric ground pressure

P_h = pressure at aircraft altitude

RC = reflection constant

M = Mach No.

VF = volume factor

LF = lift factor

WT = aircraft weight

L = " length

FR = " fineness ratio

WC = wing chord for lift distribution

II.2 OUTPUT FORMAT

The output format will be self explanatory, however to itemize:

First: problem number and aircraft data are given

Second: input atmosphere is reproduced

Third: history of shock strength variation for selected input angle is presented

Fourth: shock-ground intersection data are listed

Other possible output information is as follows:

1) If the shock is cutoff by atmospheric refraction, the location and the identification of the corresponding input angle are printed out. Also, whenever posssible, the shock overpressure at cutoff is presented.

2) If aircraft acceleration effects (that is possible high shock overpressures) take place before the shock has propagated 100 body lengths this fact is printed out.

3) If for some reason the computation to determine the pressure jump across the shock does not converge this fact is printed out.

II.3 PROGRAM LIMITATIONS

1) The aircraft altitude must be greater than ground altitude, and less than or equal to the highest altitude for which atmospheric data are prescribed.

2) The shock strength is not computed until it has propagated approximately 100 body lengths from the aircraft. To obtain data closer to the aircraft, the computer can be "fooled" by feeding in a small value for body length, L, and increasing the volume factor, VF, so that their product in Eq. (II.1) remains constant. Care should be taken when interpreting the resulting data since the present theory is essentially a far field theory. That is, the far field result would be correct but the results near the aircraft might be questionable.

3) The computation time is essentially proportional to the number of altitude steps taken to carry out the integrations times the number of input angles. The magnitude of the integration step size is one quarter of the smallest altitude spacing. For an aircraft at 60,000 ft. and altitude

data spacing 1000 ft. (step size 250 ft.) there will be about 240 integration steps; computation times on IBM 709, 7090 and 7094 are approximately 10, 2 and 1.5 seconds respectively for each input angle.

4) Basic subroutines not generally found on basic Fortran II library tapes include ASIN and TAN.

5) If ray-ground data are desired for a level-flight case, they will be computed and printed if a very small value of PSI, such as −.0000001 deg, is used with CRV = 0.0 and a finite value of TAU.

SECTION III
PROGRAM DETAILS

III.1 EQUATIONS

The basic theory is given in Ref. 1 and Section IV, however the equations actually evaluated on the computer are presented in this section. Although the equations were taken directly from the theoretical development they had to be modified slightly for evaluation on a digital computer.

All computations start at the aircraft altitude and work downward along a ray to the ground. The coordinate system used has its origin at the ground directly below the aircraft, hence the computations start at $z = h$ and end at $z = z_{ground}$.

Shock Location:

Equations for the shock location, Eq. (3.10) of Ref. 1 are integrated directly

$$\left\{ \begin{aligned} x &= \int_h^z \left[\frac{\ell V_s + u_0}{n V_s} \right] dz \\ y &= \int_h^z \left[\frac{v_0}{n V_s} \right] dz \\ t &= \int_h^z \left[\frac{1}{n V_s} \right] dz \end{aligned} \right\} \qquad \text{(III.1)}$$

After the ray-ground intersection, as determined from above equations, is computed the coordinates are referred to a fixed coordinate system by the procedure described under the heading "shock-ground intersection" later in this section.

Ray Tube Area

Since we are integrating from altitude z = h downward Eq. (IV.12) becomes, after setting $V_s dt = ds$

$$A = (h - z) \sec \nu_h \left\{ 1 - \frac{\dot{V}_a s}{a_h^2 M(M^2 - 1)} + \frac{\sec \nu_h}{V_a \cos \theta} \int_h^z \tan \nu \left[\frac{dV_s}{dz} - \sin \nu \frac{du_0}{dz} \right] dz \right\} \tag{III.2}$$

where

$$s = \int_h^z \left(\frac{ds}{dz} \right) dz \tag{III.3}$$

and (ds/dz) is given in Eq. (3.10) of Ref. 1.

Pressure Jump

There are two integrals involved in the pressure jump expression, Eq. (IV.3). The first, I(s), which is defined before Eq. (2.10) of Ref. 1, can be written

$$I(z) = \exp \left\{ \int_{z=h}^{z} \frac{\rho_0 \, dw_0 - \left[(\gamma - 1)/2 \right] w_0 \, d\rho_0}{\rho_0 \, (w_0 + a_0)} \right\} \tag{III.4}$$

This is simply an integration of atmospheric variables between aircraft altitude and altitude z. Therefore the quantity, I, can be considered as another atmospheric variable which can be derived from input data.

In order to evaluate Eq. (III.4), the density, ρ_0, was expressed in terms of pressure and sound speed

$$\frac{d\rho}{\rho} = \frac{dp}{p} - 2\frac{da}{a} \quad .$$

The second integral in the pressure jump expression

$$\int_0^s \frac{ds}{B}$$

is evaluated in the form

$$J = \int_h^z \frac{ds}{dz} \frac{dz}{B} \quad . \tag{III.5}$$

The quantity B, defined in Ref. 1, is

$$B = (a_0 + w_0)^2 \; I \left(\frac{p_0}{a_0}\right)^{1/2} A^{1/2}$$

where A is defined in Eq. (III.2). Because the ray tube area, A, vanishes at z = h, the integrand of Eq. (III.5) becomes infinite at that point. This singularity is integrable, however a little care is required to do it on a computer. First the integrand in Eq. (III.5) is written

$$\frac{1}{B} \frac{ds}{dz} = \frac{Q(z)}{\sqrt{h-z}}$$

and then the integral is written

$$J = Q(z_h) \int_h^z \frac{dz}{\sqrt{h-z}} + \int_h^z \frac{Q(z) - Q(z_h)}{\sqrt{h-z}} \, dz$$

$$= -2Q(z_h)\sqrt{h-z} + \int_h^z \frac{Q(z) - Q(z_h)}{\sqrt{h-z}}\, dz \tag{III.6}$$

By using Eq. (III.2), Eq. (3.10) of Ref. 1, and the definition of B (recalling $I(z_h) = 1$)

$$Q(z_h) = -\left[\frac{\sec \nu_h}{a_h^3\, p_h}\right]^{1/2} \tag{III.7}$$

The integrand in Eq. (III.6) now vanishes at the initial point $z = z_h$.

Aircraft Lift and Volume

The main interest in this study is to determine atmospheric and acceleration effects on shock propagation. Therefore details of the aircraft lift and volume calculations are omitted. Since the theory is asymptotic in the sense that it is applicable only at sufficient distance from the aircraft, a term which gives essentially only the far field effects of lift and volume is included.

The boom due to volume, for a uniform atmosphere, (see e.g., Eq. 44 of Ref. 2, is

$$\frac{\Delta p}{p} = \frac{(M^2-1)^{1/8}}{h^{3/4}} \cdot \left\{\int_0^{\eta_0} F(\eta)\, d\eta\right\}^{1/2} \cdot \frac{\gamma 2^{1/4}}{\sqrt{\gamma+1}}$$

$$\text{where } F(\eta) = \frac{1}{2\pi} \int_0^{\eta} \frac{S''(\xi)\, d\xi}{\sqrt{\eta-\xi}} \tag{III.8}$$

If area S is normalized with respect to $(L/FR)^2$ where L = aircraft length and FR = fineness ratio = (length/max diameter), and distance, η, measured along aircraft axis is normalized with respect to L, Eq. (III.8) can be written

$$\frac{\Delta p}{p} = \frac{(M^2-1)^{1/8}}{h^{3/4}} \quad \frac{L^{3/4}\ (VF)}{FR}$$

The volume factor VF varies, approximately, from .55 to .80, depending on the aircraft considered.

For a uniform atmosphere Eq. IV. 3 reduces to (after letting $K = K_v$)

$$\left.\frac{\Delta p}{p}\right|_{\text{volume}} = \frac{K_v (M^2 - 1)^{3/8}}{\sqrt{2}\, h^{3/4} M^{3/4}} \tag{III.9}$$

Equating the above two equations leads to

$$K_v = \frac{M^{3/4} \sqrt{2}}{(M^2 - 1)^{1/4}} \quad \frac{L^{3/4} (VF)}{FR} \tag{III.10}$$

For lifting effects (see, e.g. Eq. (49) of Ref. 3, the boom overpressure is

$$\frac{\Delta p}{p} = \frac{\gamma (M^2 - 1)^{3/8}}{2^{1/4} \sqrt{x+1}} \quad \frac{\sqrt{\cos \phi}}{h^{3/4}} \left\{ \int_0^{\eta_1} G(\eta)\, d\eta \right\}^{1/2} \tag{III.11}$$

where

$$G(\eta) = \frac{1}{2\pi} \int_0^{\eta} \frac{S''(\xi)}{\sqrt{\eta - \xi}}\, d\xi$$

and

$$S'' = \frac{d}{d\xi} \int_{\beta_1}^{\beta_2} \frac{2 \Delta p (\xi, \beta)}{\gamma p_h M^2}\, d\beta \quad .$$

The quantity S' is essentially loading along a spanwise strip, and the integration in Eq. (III.11) is a summation of the "loading sources". If the integrals in Eq. (III.11) are made dimensionless as follows

$$\Delta p = \frac{WT}{(WS)(WC)} \overline{\Delta p} = \frac{(\text{aircraft weight})}{(\text{wing span})(\text{wing chord})} \overline{\Delta p}$$

$$\beta = (WS)\,\overline{\beta}$$

$$\eta, \xi = (WC)\,\overline{\eta}, (WC)\,\overline{\xi} \text{ ; Eq. (III.11) can be written}$$

$$\frac{\Delta p}{p} = \frac{(M^2 - 1)^{3/8}}{M h^{3/4}} \frac{\sqrt{\cos\phi}}{(WC)^{1/4}} \left(\frac{WT}{p_h}\right)^{1/2} (LF) \qquad \text{(III.12)}$$

The lift factor LF varies, approximately, from .5 to .6.

Equating Eq. (III.9), with K_L instead of K_v, to Eq. (III.12) leads to

$$K_L = \frac{\sqrt{2}}{M^{1/4}} \frac{(LF)}{(WC)^{1/4}} \left(\frac{WT \cos\phi}{p_h}\right)^{1/2}$$

In order to combine the lift and volume effects, it should be noted that the integrals of F and G, in Eqs. III.8 and 11, should be added and not K_L and K_v. This can be accomplished by letting

$$K = \sqrt{K_v^2 + K_L^2}$$

$$= \sqrt{\left\{\frac{L^{3/4} \cdot VF}{FR}\right\}^2 + \cos\phi \frac{\sqrt{M^2 - 1}\,(LF)^2 \cdot WT}{M^2 \cdot p_h \cdot (WC)^{1/2}} \left[\frac{4M^3}{M^2 - 1}\right]^{.25}} \qquad \text{(III.13)}$$

The SBCP determines the pressure ratio across the shock by using Eq. IV.3, with K defined above. At the ground the pressure ratio across the shock is multiplied by a reflection constant, RC, which equals 1.8 – 2.0, approximately.

Shock-Ground Intersection

As indicated in Ref. 1, the origin of the ray coordinate system must move with the wind at aircraft altitude. The ray-ground intersection (x_g, y_g) are related to fixed (aircraft wind) axes through Eqs. (3.13) and (3.14) of Ref. 1:

$$
\begin{aligned}
X_g &= x_g \cos\theta - y_g \sin\theta + U_h t_g \\
Y_g &= x_g \sin\theta + y_g \cos\theta + V_h t_g \\
t_g &= \text{time for ray to reach ground} \\
V_h &= \text{headwind at aircraft altitude} \\
V_h &= \text{sidewind at aircraft altitude}
\end{aligned}
\qquad \text{(III.14)}
$$

The aircraft ground speed, V_g, is given by

$$V_g = \sqrt{(V_a - U_h)^2 + V_h^2}$$

The vertex of the shock is given by the coordinates of ray $\phi = 0$, directly below the aircraft, and other points on the shock are determined by projecting back the remaining ray-ground intersection points. Since the fixed coordinate system, to which all this is referred, is aligned with the aircraft air velocity vector and not the ground speed vector the projection is carried out as follows:

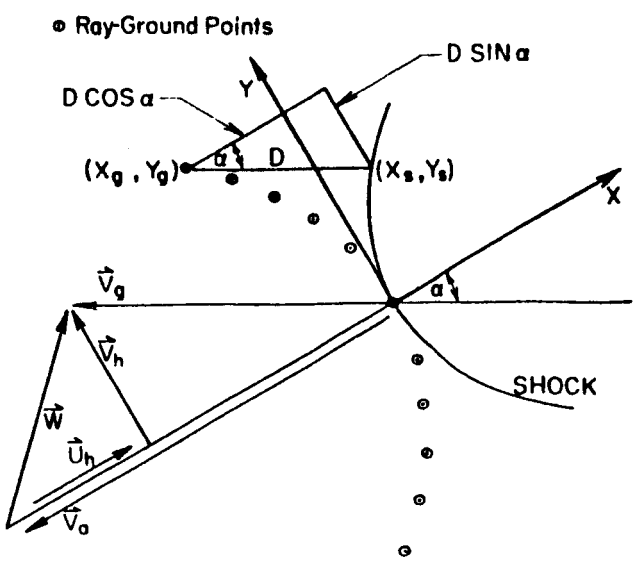

The shock maintains its shape (changes in Mach number due to acceleration are neglected) as it moves in the V_g direction. Therefore points on the shock (X_s, Y_s) are related to ray points by projecting back the distance D as indicated in Eq. (3.15) in Ref. 1. The relations are

$$X_s = X_g + D \cos \alpha$$

$$Y_s = Y_g - D \sin \alpha \qquad \text{(III.15)}$$

$$\tan \alpha = \frac{V_h}{V_a - U_h}$$

III. 2 PROGRAM SYMBOLS (FORTRAN)

The altitudes are numbered: highest altitude, K = 1; lowest altitude, K = KEND = first number on control card. The atmospheric variables are

Z (1,K) { = initially, temperature, readin for computation of sound speed
= w_0, Eq. (3.2) in Ref. 1

Z (2, K) = pressure, p_0

Z (3, K) = sound speed, a_0

Z (4, K) = relative wind along x axis, u_0

Z (5, K) = relative wind along y axis, v_0

Z (6, K) = I, Eq. (III.4)

Z (7, K) = altitude

Z (8, K) = aircraft headwind

Z (9, K) = aircraft sidewind

S (J), J = 1 to 9 = values of the above Z variables obtained by interpolating between two input altitudes

The angles are numbered in the order that they were entered onto the input angle cards. N = 1, corresponds to the first angle, . . . , N = NEND (second entry on control card), corresponds to the last angle. In the SBCP the angles are denoted

PHI (N) N = 1 to NEND

DATA (N,J, MP) are output data corresponding to angle N

DATA (N,1, MP) = pressure jump across shock

DATA (N,2, MP) = X shock coordinate

DATA (N,3, MP) = Y shock coordinate

DATA (N,4, MP) = shock propagation time between aircraft and ground

W(1), X(1), Y(1), AY(1) = parameters for evaluating Eq. (III.5)

W (2), X(2), Y (2), AY(2) = parameters for evaluating Eq. (III.1) first eqn.

W (3), X(3), Y(3), AY(3) = parameters for evaluating Eq. (III.1) second eqn.

W (4), X(4), Y(4), AY(4) = parameters for evaluating Eq. (III.1) third eqn.

W (5), X(5), Y(5), AY(5) = parameters for evaluating aircraft acceleration term in Eq. (III.2)

W (6), X(6), Y(6), AY(6) = parameters for evaluating the last integral in Eq. (III.2)

PJ (1)	=	altitude of point on ray path
PJ (2)	=	X coordinate of point on ray path
PJ (3)	=	Y coordinate of point on ray path
PJ (4)	=	shock pressure ratio of point on ray path
PJ (5)	=	shock pressure jump of point on ray path
PJ (6)	=	atmospheric pressure of point on ray path
ACC	=	aircraft acceleration
AF	=	ray tube area Eq. (III.2)
ALT	=	aircraft altitude
APR	=	previous pressure ratio
AVS	=	shock velocity
B	=	a parameter
BONG	=	aircraft length
BSA	=	aircraft lift term
BSC	=	aircraft shape term Eq. (III.13) without Mach number term
BSV	=	aircraft volume term
C	=	Snell's constant $= - \lvert V_a \rvert \cos \theta$
C1	=	acceleration and curvature contribution, Eq. (AIV.13)
C2	=	$BSC \cdot (4M^3/(M^2 - 1))^{.25}$
DL	=	integration step size
EL	=	ray x direction cosine
ELH	=	x direction cosine of ray, initially
EM	=	aircraft Mach number
EN	=	ray y direction cosine
FL	=	lift factor
G	=	$(a_h^3 \, p_h)^{-1/4}$ = Eq. (IV.5)
H	=	the negative of the y direction cosine of the ray, initially
HH	=	1/H
NN	=	number corresponding to angle for output data
NV	=	number corresponding to angle $\phi = 0$
PR	=	pressure ratio
Q(J), J = 1, 5	=	parameters

RC	=	shock-ground reflection constant
R1	=	$Q(z_a)$ in Eq. (III.7)
R2	=	$-(ds/dz)$
STH	=	$\sin \theta$
T	=	aircraft fineness ratio
TEST	=	a parameter
U	=	wind speed, u_0
VF	=	volume factor
VP	=	derivative of shock velocity
VS	=	shock velocity
WL	=	aircraft wing chord
WT	=	aircraft wieght

III.3 SUBROUTINES

In this subsection the various parts of the SBCP will be discussed. The program consists of a main part with eight subroutines.

SUBROUTINE ALTA

The first subroutine encountered is called ALTA. There is a restriction on the input data, that is the aircraft altitude must be greater than the ground and less than or equal to the highest atmospheric data point. As the atmospheric data is read in by the computer, highest altitude first, they are numbered in sequential order. In subroutine ALTA the location of the aircraft altitude relative to the input altitude sequence is determined. The aircraft altitude is then made the first altitude in the sequence and all atmospheric data sequences are re-numbered starting at the aircraft altitude and going down to the ground.

SUBROUTINE ONE

In this subroutine initial conditions for all integrations are determined. Also, wind components relative to the ray coordinate system (see Ref. 1) are computed. In addition, the variable I (z) given in Eq. (III.4) is determined.

SUBROUTINE MID

All integrations are carried out by using the trapezoidal method. Some integration points fall at altitudes between the input altitudes. In subroutine MID a linear interpolation is carried out to determine atmospheric data at the points between the tabulated altitudes.

SUBROUTINE LINT

In this and the following two subroutines the integrations which are required for location of the shock and determination of the pressure jump across the shock are carried out. For the first 100 body lengths from the aircraft only the shock location is determined; some of the integrations involved in the pressure jump expression are carried out, however no shock overpressures are computed. Since the shock overpressure is not computed the true shock velocity is not known; therefore, in this initial region it is assumed that the shock propagates at acoustic speed.

The integrations over the first 100 body lengths are carried out in subroutines LINT and FIN. In LINT the integrals are evaluated by means of the trapezoidal method, with a step size equal to the spacing of input atmospheric data. This is carried out to the input altitude which is just above the altitude 100 body lengths from the aircraft.

If the aircraft altitude is the only input data point above that altitude which is 100 body lengths below the aircraft, subroutine LINT is bypassed. For this case the integration over the first 100 body lengths is carried out in subroutine FIN.

SUBROUTINE FIN

In this subroutine the shock location and overpressure integrals are evaluated between the altitude 100 body lengths from the aircraft and the input altitude immediately above it. Upon completion of this integration shock overpressure and velocity are computed for the first time.

At the end of this subroutine the step size for the remaining integrations, which continue until the ground is reached, is computed. This step size is set at one quarter of the smallest input altitude spacing.

SUBROUTINE INTEG

The shock location and overpressure integrals are determined in this subroutine using actual shock velocities. In order to do this an iteration process has been introduced, this is because the overpressure integrals is of the form.

$$p(z) = \int_h^z f(z, p(z))\, dz$$

$$\cong \int_h^{z-\Delta z} f(z, p)\, dz + \frac{\Delta z}{2} \left(f(z, p(z)) + f(z-\Delta z,\ p(z-\Delta z))\right)$$

Since the pressure at the point to be computed is on both the right and left hand sides of the above equation an iteration process is required to determine it. When two successive pressures, at a given point, agree to within one percent this value is assumed to be the correct value.

It can be shown (Ref. 4) that a more accurate expression for the ray tube area than that given in Eq. III.2 involves integrals along the shock front. A limitation of the present ray tube approach is that it assumes flow properties in each ray tube to be independent of properties in adjacent ray tubes. Therefore integrals along the shock front, through ray tubes, are not possible. The effect of these (omitted) integrals is to cause a buildup of ray tube area in opposition to a decrease in ray tube area such as would occur for an accelerating aircraft. However these integrals are only important when the shock front curvature is large, which occurs near the "cusp point" on the shock front. At this point these integrals increase in value until they cancel the aircraft acceleration term in the ray tube area expression, Eq. II.2. This behavior is taken care of in the SBCP by setting the aircraft acceleration term equal to zero at, or near the cusp point.

MAIN PROGRAM

In this part of the SBCP input, output and certain decision making operations are carried out. The most important of the decisions made is that associated with the iteration to determine the shock overpressure, described under SUBROUTINE INTEG above. This iteration is carried out

12 times. If, after this, the pressures still do not agree to within one percent the integration step size is cut in half and the procedure is started over again. This is continued, if necessary, until the integration step size is 5 feet or less. When this occurs the computation stops as there is something wrong, either with the theory, the data, or the computer.

Acoustical cutoff is assumed to occur when the shock front is within approximately 2.5 degrees of being normal to the horizontal direction. If this occurs within 100 body lengths of the aircraft, the altitude and the ray direction being considered is printed out. If cutoff occurs below 100 body lengths from the aircraft shock overpressure data is also printed out.

The last thing the program does is to compute the ground-shock data. After this is printed out the program either stops or reads in new data if there is any (last entry on control card).

SUBROUTINE CORR

Here the location of the second flight path point used for climbing or diving curved maneuvers is determined. As described in Appendix IV, this point is necessary for locating the ground-shock intersection.

SUBROUTINE SORT

In this subroutine, used only for diving and climbing flight paths, the ground-shock intersection is determined. Also, the results of the computation are printed out. The details are given in Appendix IV.

FUNCTION SUBROUTINES

ASIN	EXP
SIN	EXP(3
COS	MIN 1
SQRT	SIGN
TAN	

SECTION IV

IMPROVEMENTS TO THE THEORY

The general theory is given in Ref. 1, however, since the publication of that theory several improvements have been made. These improvements are given in this section.

IV.1 THE PRESSURE JUMP EXPRESSION

There is a certain amount of arbitrariness in the dimensional scaling of the pressure jump expression, Eq. (2.16) of Ref. 1. A more detailed discussion will be given here.

Equation (2.13) of Ref. 1 can be written

$$L = \frac{L_0 \left\{ \int_0^s \frac{ds}{B(s)} \right\}^{1/2}}{\left\{ \int_0^{s_0} \frac{ds}{B(s)} \right\}^{1/2}} \tag{IV.1}$$

That is $L = L_0$ when $s = s_0$. The natural initial condition, $L = 0$ at $s = 0$, is automatically taken care of by the above solution. (The differential equation for L is singular at the initial point, hence the initial point cannot be used to prescribe initial conditions.)

Substituting the above result into the top line of Eq. (2.14), Ref. 1

$$\frac{p - p_0}{p_0} = \frac{\frac{2\gamma}{\gamma + 1} L_0}{a_0 \, I(s) \left\{ \int_0^{s_0} \frac{ds}{B(s)} \right\}^{1/2} \left\{ \int_0^{s} \frac{ds}{B(s)} \right\}^{1/2} \left\{ \frac{Ap}{a_0} \right\}^{1/2}} \tag{IV.2}$$

To determine L_0 we assume a uniform atmosphere and equate Eq. (IV.2) to Eq. (2.15), Ref. 1

$$\frac{2\gamma}{\gamma + 1} L_0 = \frac{K}{a_0} \left\{ \int_0^{s_0} \frac{ds}{\sqrt{A}} \right\}^{1/2}$$

Therefore

$$\frac{p - p_0}{p_0} = \frac{K}{G(s_0)\, a_0^2\, I(s) \left\{ \frac{Ap}{a_0} \right\}^{1/2} \left\{ \int_0^s \frac{ds}{B(s)} \right\}^{1/2}} \quad , \qquad \text{(IV.3)}$$

where

$$G(s_0) = \left[\frac{\int_0^{s_0} \frac{ds}{B(s)}}{\int_0^{s_0} \frac{ds}{\sqrt{A}}} \right]^{1/2}$$

It should be noted that $G(s_0)$ depends on the quantity s_0 which has not yet been determined. By letting

$$\sigma = \int_0^s \frac{ds}{\sqrt{A}} \quad , \quad d\sigma = \frac{ds}{\sqrt{A}}$$

we have

$$G(\sigma_0) = \left\{ \frac{1}{\sigma_0} \int_0^{\sigma_0} \frac{d\sigma}{(a_0 + w_0)^2\, I\, \{ p/a_0 \}^{1/2}} \right\}^{1/2} \qquad \text{(IV.4)}$$

$$= \left\{ \text{average over distance } \sigma_0 \right\}^{1/2}$$

By letting σ_0 approach zero, or the aircraft altitude, $w_0 = 0$, $I = 1$, we obtain

$$G \equiv G(0) = 1/(a_h^3\, p_h)^{1/4} \qquad \text{(IV.5)}$$

It has been found that using the value of G given in Eq. (IV.5) leads to good agreement with field test data. Therefore, Eq. (IV. 3) has been used in the SBCP with $G(s_0)$ defined in Eq. (IV.5).

By using the approach described in this section, one need not start off with dimensionless variables, as described below Eq. (2.1), Ref. 1.

IV.2 RAY TUBE AREA

The derivation of an expression for the ray tube area, given in Part 4 of Ref. 1, has been improved. It was found that Eq. (4.4) was too crude and a better approximation is given below

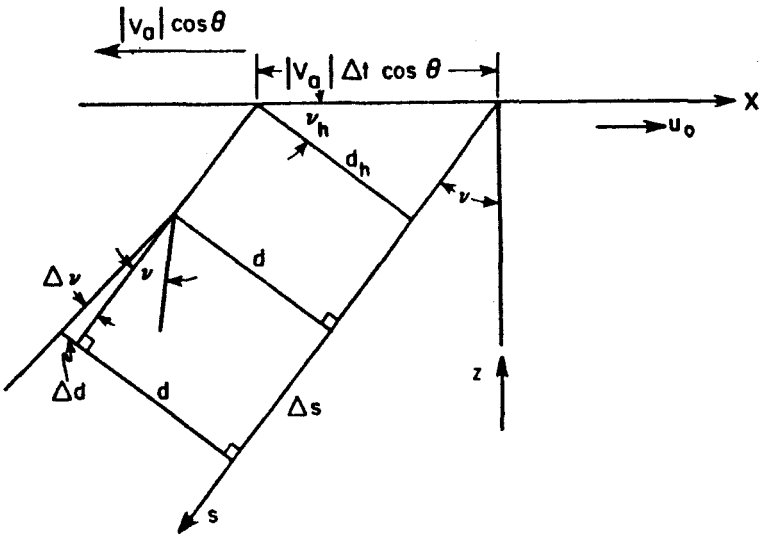

The change in distance between rays, Δd, due to a change in slope, $\Delta\nu$, in a distance Δs along the ray is

$$\Delta d = \Delta\nu \Delta s$$

Integrating this along the ray

$$d = d_h + \int_0^s \Delta\nu \, ds \qquad \text{(IV.6)}$$

where $d_h = |V_a| \Delta t \cos\theta \cos\nu_h$ (IV.7)

The quantity $\Delta\nu$ will be considered to be made up of two parts

$$\Delta\nu = \Delta_1 \nu + \Delta_2 \nu \qquad \text{(IV.8)}$$

The first part, $\Delta_1 \nu$, is the initial difference between the slope of the two rays caused by aircraft acceleration. The second part, $\Delta_2 \nu$, is a change

in slope due to the interrelation between the shock strength and ray tube area.

Using Eq. (3.9) of Ref. 1, at the aircraft altitude, assuming $V_s = a_h$

$$\sin \nu = \frac{a_h}{V_a \cos \theta} ,$$

and hence

$$\Delta_1 \nu = - \Delta V_a \frac{\cos \phi \cos \theta}{a_h M \sqrt{M^2 - 1}} \tag{IV.9}$$

Variations along the ray are given by $\Delta_2 \nu$, this is determined from

$$\sin \nu = \frac{V_s}{V_a \cos \theta + u_0}$$

and leads to

$$\Delta_2 \nu = \tan \nu \left[\frac{\Delta V_s}{V_s} - \sin \nu \frac{\Delta u_0}{V_s} \right] \tag{IV.10}$$

As in Ref. 1, Part 4, we let

$$A \sim z d \tag{IV.11}$$

Combining Eqs. (IV.6 – 11), we obtain after some algebraic simplification of the acceleration term

$$A = z \sec \nu_h \left\{ 1 - \frac{\dot{V}_a S}{a_h^2 M (M^2 - 1)} + \frac{\sec \nu_h}{V_a \cos \theta} \int_0^s \frac{\tan \nu}{V_s} \left[\frac{dV_s}{dt} - \sin \nu \frac{du_0}{dt} \right] ds \right\} \tag{IV.12}$$

Actually, a different approach based on the theory given in Ref. 4 will give a more correct result. However because of the complexity of that approach it is felt that its inclusion is not justified at this time. An attempt is now being made to simplify this theory in order to incorporate it into the present ray tube approach.

APPENDIX I

REFERENCES

1. Friedman, M. P., Kane, E. J., Sigalla, A., "Effects of Atmosphere and Aircraft Motion on the Location and Intensity of a Sonic Boom", AIAA Journal, Vol. 1, p. 1327, June 1963.

2. Whitham, G. B., "The Flow Pattern of a Supersonic Projectile", Comm. Pure and Appl. Math., Vol. V, p. 301, August 1952.

3. Walkden, F., "The Shock Pattern of a Wing-Body Combination, Far from the Flight Path", Aero. Quart., Vol. IX, p. 164, May 1958.

4. Whitham, G. B., "A New Approach to Problems of Shock Dynamics, Part 1, Two-dimensional Problems", J. Fl. Mech., Vol. 2, p.145, 1957.

APPENDIX II
TWO SAMPLE PROBLEMS

In this section the input and output for two sample problems will be given. The first problem, case 1001, involves a low Mach number (M = 1.1) aircraft flying at 40,000 ft. and accelerating at 4 ft./sec^2; the atmosphere is an ICAO 1959 standard atmosphere. The second problem, case 0000, has a Mach 2 aircraft flying at 60,000 ft. in a constant atmosphere. The input cards for both problems are indicated as follows:

A: control card
B: atmosphere cards
C: angle card
D: aircraft data cards

Because of atmospheric refraction due to changes in temperature with altitude, the shock does not get to the ground in case 1001. There are, however, quite a few interesting results. The acceleration causes a peak overpressure at 16650 feet for the zero angle ray. This phenomenon occurs at similar altitudes for the other angle rays.

```
        16          7        1001          4          4  } A
70.        93.672    -69.61
65.       118.93     -69.61
60.       151.03     -69.61
55.       191.80     -69.61
50.       243.61     -69.61
45.       309.45     -69.61
40.       393.12     -69.61
35.       499.34     -65.52
30.       629.66     -47.74                  } B
25.       786.33     -29.96
20.       973.27     -12.17
15.       1194.8     5.63
10.       1455.6     23.44
 5.       1760.9     41.26
 1.       2040.9      55.43
 0.       2116.2     59.09
   -45.      -30.      -15.      0.       15.       30.       45.  } C
4.0       100.0       1.8       1.1       40000.    .64        .6  } D
 100000.     8.       50.
        3          4        0000          2          1         -1  } A
 60.       657.6      -44.4
  8.       657.6      -44.4                  } B
  0.       657.6      -44.4
 -30.      0.        15.        30.  } C
 0.        100.       1.8       2.0       60000.    .64        0.  } D
 100000.     8.        50.
```

SONIC BOOM, CASE 1001, M= 1.100, ALTITUDE= 40000., ACC= 4.000, RC=1.80, VF= 0.640, LF= 0.600
WT= 100000.0, LENGTH= 100.0, FR= 8.00, WL=50.000

ALTITUDE (FT)	HEADWIND (FPS)	SIDEWIND (FPS)	PRESSURE (PSF)	SOUND SPEED (FPS)	TEMPERATURE (DEG F)
70000.	-0.	-0.	93.672	967.660	-69.610
65000.	-0.	-0.	118.930	967.660	-69.610
60000.	-0.	-0.	151.030	967.660	-69.610
55000.	-0.	-0.	191.800	967.660	-69.610
50000.	-0.	-0.	243.610	967.660	-69.610
45000.	-0.	-0.	309.450	967.660	-69.610
40000.	-0.	-0.	393.120	967.660	-69.610
35000.	-0.	-0.	499.340	972.721	-65.520
30000.	-0.	-0.	629.660	994.422	-47.740
25000.	-0.	-0.	786.330	1015.660	-29.960
20000.	-0.	-0.	973.270	1036.475	-12.170
15000.	-0.	-0.	1194.800	1056.890	5.630
10000.	-0.	-0.	1455.600	1076.930	23.440
5000.	-0.	-0.	1760.900	1096.615	41.260
1000.	-0.	-0.	2040.900	1112.019	55.430
0.	-0.	-0.	2116.200	1115.964	59.090

CUTOFF ALTITUDE, ANGLE=-45.00

Z (FT)	X (FT)	Y (FT)	PRESSURE RATIO	PRESSURE JUMP (PSF)	PRESSURE (PSF)
26108.	-66218.	21457.	0.0026115	1.963	751.605

CUTOFF ALTITUDE, ANGLE=-30.00

Z (FT)	X (FT)	Y (FT)	PRESSURE RATIO	PRESSURE JUMP (PSF)	PRESSURE (PSF)
20433.	-80315.	18402.	0.0048093	4.603	957.070

CUTOFF ALTITUDE, ANGLE=-15.00

Z (FT)	X (FT)	Y (FT)	PRESSURE RATIO	PRESSURE JUMP (PSF)	PRESSURE (PSF)
15133.	-98920.	11732.	0.0003973	0.472	1188.913

HISTORY OF SHOCK STRENGTH VARIATION, ANGLE= 0.

Z (FT)	X (FT)	Y (FT)	PRESSURE RATIO	PRESSURE JUMP (PSF)	PRESSURE (PSF)
29750.	-23916.	-0.	0.0028460	1.814	637.493
29500.	-24582.	-0.	0.0028199	1.820	645.327
29250.	-25253.	-0.	0.0027816	1.817	653.160
29000.	-25929.	-0.	0.0027383	1.810	660.994
28750.	-26611.	-0.	0.0026937	1.802	668.827
28500.	-27299.	-0.	0.0026494	1.793	676.661
28250.	-27993.	-0.	0.0026064	1.784	684.494
28000.	-28693.	-0.	0.0025651	1.776	692.328
27750.	-29400.	-0.	0.0025257	1.768	700.161
27500.	-30114.	-0.	0.0024881	1.762	707.995
27250.	-30834.	-0.	0.0024525	1.756	715.828
27000.	-31562.	-0.	0.0024187	1.750	723.662
26750.	-32296.	-0.	0.0023866	1.746	731.495
26500.	-33039.	-0.	0.0023564	1.742	739.329
26250.	-33788.	-0.	0.0023278	1.739	747.162
26000.	-34546.	-0.	0.0023008	1.737	754.996
25750.	-35312.	-0.	0.0022755	1.736	762.829
25500.	-36087.	-0.	0.0022517	1.735	770.663
25250.	-36870.	-0.	0.0022295	1.736	778.496
25000.	-37661.	-0.	0.0022088	1.737	786.330
24750.	-38463.	-0.	0.0021882	1.741	795.677
24500.	-39273.	-0.	0.0021692	1.746	805.024
24250.	-40093.	-0.	0.0021517	1.752	814.371
24000.	-40923.	-0.	0.0021359	1.759	823.718
23750.	-41764.	-0.	0.0021217	1.768	833.065
23500.	-42615.	-0.	0.0021092	1.777	842.412

23250.	-43477.	-0.	0.0020984	1.787	851.759
23000.	-44351.	-0.	0.0020894	1.799	861.106
22750.	-45236.	-0.	0.0020823	1.813	870.453
22500.	-46134.	-0.	0.0020770	1.827	879.800
22250.	-47045.	-0.	0.0020739	1.844	889.147
22000.	-47970.	-0.	0.0020729	1.862	898.494
21750.	-48908.	-0.	0.0020742	1.883	907.841
21500.	-49861.	-0.	0.0020781	1.906	917.188
21250.	-50829.	-0.	0.0020849	1.932	926.535
21000.	-51814.	-0.	0.0020947	1.960	935.882
20750.	-52815.	-0.	0.0021080	1.993	945.229
20500.	-53834.	-0.	0.0021252	2.029	954.576
20250.	-54872.	-0.	0.0021471	2.070	963.923
20000.	-55929.	-0.	0.0021742	2.116	973.270
19750.	-57007.	-0.	0.0022064	2.172	984.346
19500.	-58107.	-0.	0.0022467	2.236	995.423
19250.	-59230.	-0.	0.0023083	2.323	1006.499
19000.	-60378.	-0.	0.0023645	2.406	1017.576
18750.	-61553.	-0.	0.0024559	2.526	1028.652
18500.	-62756.	-0.	0.0025621	2.664	1039.729
18250.	-63989.	-0.	0.0026971	2.834	1050.805
18000.	-65257.	-0.	0.0028764	3.054	1061.882
17750.	-66561.	-0.	0.0031440	3.373	1072.958
17700.	-66829.	-0.	0.0031561	3.393	1075.174
17650.	-67100.	-0.	0.0030880	3.327	1077.389
17600.	-67375.	-0.	0.0030795	3.325	1079.604
17550.	-67652.	-0.	0.0031048	3.359	1081.820
17500.	-67931.	-0.	0.0031507	3.416	1084.035
17450.	-68212.	-0.	0.0032105	3.487	1086.250
17400.	-68495.	-0.	0.0032966	3.588	1088.466
17350.	-68780.	-0.	0.0033649	3.670	1090.681
17300.	-69068.	-0.	0.0034656	3.788	1092.896
17250.	-69357.	-0.	0.0035475	3.885	1095.111
17200.	-69650.	-0.	0.0036691	4.026	1097.327
17150.	-69944.	-0.	0.0037871	4.164	1099.542
17100.	-70241.	-0.	0.0039142	4.313	1101.757
17050.	-70541.	-0.	0.0040545	4.476	1103.973
17000.	-70844.	-0.	0.0042101	4.657	1106.188
16950.	-71150.	-0.	0.0043828	4.858	1108.403
16900.	-71459.	-0.	0.0045746	5.081	1110.619
16850.	-71772.	-0.	0.0047874	5.328	1112.834
16800.	-72088.	-0.	0.0050230	5.601	1115.049
16750.	-72407.	-0.	0.0052827	5.902	1117.264
16700.	-72731.	-0.	0.0055668	6.232	1119.480
16650.	-73060.	-0.	0.0058748	6.590	1121.695
16600.	-73384.	-0.	0.0004907	0.552	1123.910
16550.	-73700.	-0.	0.0004897	0.551	1126.126
16500.	-74013.	-0.	0.0004884	0.551	1128.341
16250.	-75590.	-0.	0.0004832	0.551	1139.417
16000.	-77207.	-0.	0.0004763	0.548	1150.494
15750.	-78879.	-0.	0.0004687	0.544	1161.570
15500.	-80623.	-0.	0.0004607	0.540	1172.647
15250.	-82452.	-0.	0.0004526	0.536	1183.723
15000.	-84383.	-0.	0.0004444	0.531	1194.800
14750.	-86435.	-0.	0.0004360	0.527	1207.840
14500.	-88635.	-0.	0.0004275	0.522	1220.880
14250.	-91019.	-0.	0.0004169	0.514	1233.920
14000.	-93642.	-0.	0.0004094	0.510	1246.960
13750.	-96596.	-0.	0.0004012	0.506	1260.000
13500.	-100051.	-0.	0.0003903	0.497	1273.040
13250.	-104416.	-0.	0.0003819	0.491	1286.080

CUTOFF ALTITUDE, ANGLE= 0.

Z (FT)	X (FT)	Y (FT)	PRESSURE RATIO	PRESSURE JUMP (PSF)	PRESSURE (PSF)
13242.	-104572.	-0.	0.0003773	0.485	1286.487

CUTOFF ALTITUDE, ANGLE= 15.00

Z (FT)	X (FT)	Y (FT)	PRESSURE RATIO	PRESSURE JUMP (PSF)	PRESSURE (PSF)
15133.	-98921.	-11733.	0.0003972	0.472	1188.913

CUTOFF ALTITUDE, ANGLE= 30.00

Z (FT)	X (FT)	Y (FT)	PRESSURE RATIO	PRESSURE JUMP (PSF)	PRESSURE (PSF)
20433.	-80314.	-18402.	0.0048083	4.602	957.070

CUTOFF ALTITUDE, ANGLE= 45.00

Z (FT)	X (FT)	Y (FT)	PRESSURE RATIO	PRESSURE JUMP (PSF)	PRESSURE (PSF)
26108.	-66215.	-21456.	0.0026088	1.961	751.605

SONIC BOOM, CASE 1001, M= 1.100, ALTITUDE= 40000.

SHOCK-GROUND DATA

ANGLE (DEG)	PRESSURE JUMP (PSF)	X (FT)	Y (FT)	TIME (SEC)
-45.00	0.	0.	0.	-1.00
-30.00	0.	0.	0.	-1.00
-15.00	0.	0.	0.	-1.00
0.	0.	0.	0.	-1.00
15.00	0.	0.	0.	-1.00
30.00	0.	0.	0.	-1.00
45.00	0.	0.	0.	-1.00

SONIC BOOM, CASE 0, M= 2.000, ALTITUDE= 60000., ACC= 0. , RC=1.80, VF= 0.640, LF= 0.
WT= 100000.0, LENGTH= 100.0, FR= 8.00, WL=50.000

ALTITUDE (FT)	HEADWIND (FPS)	SIDEWIND (FPS)	PRESSURE (PSF)	SOUND SPEED (FPS)	TEMPERATURE (DEG F)
60000.	-0.	-0.	657.600	998.446	-44.400
8000.	-0.	-0.	657.600	998.446	-44.400
0.	-0.	-0.	657.600	998.446	-44.400

HISTORY OF SHOCK STRENGTH VARIATION, ANGLE=-30.00

Z (FT)	X (FT)	Y (FT)	PRESSURE RATIO	PRESSURE JUMP (PSF)	PRESSURE (PSF)
49340.	-7108.	6156.	0.0024984	1.643	657.600
47340.	-8444.	7313.	0.0022029	1.449	657.600
45340.	-9780.	8470.	0.0019716	1.297	657.600
43340.	-11116.	9626.	0.0017893	1.177	657.600
41340.	-12451.	10783.	0.0016420	1.080	657.600
39340.	-13786.	11939.	0.0015202	1.000	657.600
37340.	-15121.	13095.	0.0014176	0.932	657.600
35340.	-16456.	14251.	0.0013362	0.879	657.600
33340.	-17790.	15407.	0.0012609	0.829	657.600
31340.	-19125.	16563.	0.0011938	0.785	657.600
29340.	-20460.	17719.	0.0011342	0.746	657.600
27340.	-21794.	18874.	0.0010811	0.711	657.600
25340.	-23129.	20030.	0.0010335	0.680	657.600
23340.	-24463.	21186.	0.0009904	0.651	657.600
21340.	-25798.	22341.	0.0009514	0.626	657.600
19340.	-27132.	23497.	0.0009157	0.602	657.600
17340.	-28466.	24652.	0.0008830	0.581	657.600
15340.	-29800.	25808.	0.0008529	0.561	657.600
13340.	-31135.	26963.	0.0008252	0.543	657.600
11340.	-32469.	28119.	0.0007994	0.526	657.600
9340.	-33803.	29274.	0.0007754	0.510	657.600
7340.	-35137.	30430.	0.0007569	0.498	657.600
5340.	-36471.	31585.	0.0007331	0.482	657.600
3340.	-37805.	32740.	0.0007164	0.471	657.600
1340.	-39139.	33896.	0.0006951	0.457	657.600
0.	-40033.	34670.	0.0006844	0.450	657.600

SONIC BOOM, CASE 0, M= 2.000, ALTITUDE= 60000.

SHOCK-GROUND DATA

ANGLE (DEG)	PRESSURE JUMP (PSF)	X (FT)	Y (FT)	TIME (SEC)
-30.00	0.810	-18569.	34670.	80.12
0.	0.901	-34663.	0.	69.37
15.00	0.876	-30994.	-16088.	71.82
30.00	0.810	-18569.	-34669.	80.12

APPENDIX III

FORTRAN LISTING

```
*       LIST8
*       LABEL
*      SYMBOL TABLE
       SUBROUTINE ALTA
       DIMENSION Z(9,100),S(9),W(9),X(9),Y(9),PJ(7),Q(9),AY(9),DATA(21,5,
      1 2),PHI(21)
       COMMON Z,KEND,CTH,STH,C,B,S,G,KQ,DL,H,R1,W,X,C1,Y,F,VS,VP,C2,AY,PJ
      1,BSV,BSA,PHI,DATA,PR,U,AVS,JNR,NEND,ALT,EL,Q,EZ,BSC,ELH,KASE,EM,EN
      1,N,ACC,RC,BONG,NV,NN,JOBS,WT,T,WL,VF,FL,APR,BVP,TEST,AF,HH
        DO 50 K=1,KEND
        IF(ALT-Z(7,K)) 50,50,51
 50     CONTINUE
 51     KA=K
        R=(ALT-Z(7,KA))/(Z(7,KA-1)-Z(7,KA))
        DO 52 J=1,9
        Z(J,1)=Z(J,KA)+R*(Z(J,KA-1)-Z(J,KA))
        DO 53 K=KA,KEND
        KK=K-KA+2
 53     Z(J,KK)=Z(J,K)
 52     CONTINUE
        KEND=KEND-KA+2
       G=(Z(3,1)/Z(2,1))**.25/Z(3,1)
       BSV=VF/T*BONG**.75
       BSA=FL*SQRTF(WT/Z(2,1)/SQRTF(WL))
        RETURN
        END
```

```
*       LIST8
*       LABEL
*       SYMBOL TABLE
        SUBROUTINE ONE
        DIMENSION Z(9,100),S(9),W(9),X(9),Y(9),PJ(7),Q(9),AY(9),DATA(21,5,
       1 2),PHI(21)
        COMMON Z,KEND,CTH,STH,C,B,S,G,KQ,DL,H,R1,W,X,C1,Y,F,VS,VP,C2,AY,PJ
       1,BSV,BSA,PHI,DATA,PR,U,AVS,JNR,NEND,ALT,EL,Q,EZ,BSC,ELH,KASE,EM,EN
       1,N,ACC,RC,BONG,NV,NN,JOBS,WT,T,WL,VF,FL,APR,BVP,TEST,AF,HH
         COMMON CRV,PSI,TAU, PS,TS,XD,YD,ZD ,VT,MP
        EZ=0.
        B=EM*EM-1.
         BQ=SQRTF(B)
        D=SINF(PHI(N)/57.2958)
         DQ=SQRTF(1.0-D*D)
         BSC=SQRTF(BSV**2+BSA**2*DQ*BQ/(B+1.0))
         CPS=COSF(PSI/57.2958)
         SPS=SINF(PSI/57.2958)
 11      AA=SQRTF(D*D+(CPS/BQ+DQ*SPS)**2)
         STH=D/AA
         CTH=SQRTF(1.0-STH**2)
         ELH=-BQ*AA/EM
        H=SQRTF(1.-ELH*ELH)
         HH=1.0/H
        C=Z(3,1)/ELH
         BJ=ACC/(Z(3,1)*EM)**2/B/ELH/CTH
         BK=1.0-SPS*(SPS-CPS*DQ*BQ)/H/H
         BL=BJ*BK
         BM=CRV*DQ/EM/H/H
         BN=SPS*DQ-BQ*CPS+STH*D/CTH
         BP=BM*BN
 12      C1=BP-BL
        C2=1.414*BSC*(EM**3/B)**.25
   14 R1=1./(Z(3,1)**1.5*SQRTF(Z(2,1)*H))
         DO 15 M=1,6
 15     Y(M)=0.
        W(1)=0.
        W(2)=-ELH/H
        W(3)=0.
        W(4)=-1./(Z(3,1)*H)
         W(5)=C1/H/H
        Z(4,1)=0.
        Z(5,1)=0.
        Z(1,1)=0.
        Z(6,1)=1.
        DO 8 K=2,KEND
        Z(4,K)=CTH*(Z(8,K)-Z(8,1))+STH*(Z(9,K)-Z(9,1))
        Z(5,K)=CTH*(Z(9,K)-Z(9,1))-STH*(Z(8,K)-Z(8,1))
        B=Z(4,K)*Z(3,K)**2/(C-Z(4,K))
        V=Z(4,K)**2+Z(5,K)**2
        Z(1,K)=(B+V)/SQRTF(Z(3,K)**2+V+2.*B)
        DO 5 I=1,3
 5      S(I)=.5*(Z(I,K)+Z(I,K-1))
        B=Z(1,K)-Z(1,K-1)
        V=(Z(2,K)-Z(2,K-1))/S(2)
        F=2.*(Z(3,K)-Z(3,K-1))/S(3)
 8      Z(6,K)=Z(6,K-1)*EXPF((B-.2*S(1)*(V-F))/(S(1)+S(3)))
         Q(1)=(Z(3,2)+Z(1,2)-Z(3,1))/(Z(7,2)-Z(7,1))
   13    W(6)=Q(1)*ELH/C/H/H
        DO 16 KZ=1,9
   16 Q(KZ)=0.
        RETURN
        END
```

```
*       LIST8
*       LABEL
*       SYMBOL TABLE
        SUBROUTINE MID
        DIMENSION Z(9,100),S(9),W(9),X(9),Y(9),PJ(7),Q(9),AY(9),DATA(21,5,
       1 2),PHI(21)
        COMMON Z,KEND,CTH,STH,C,B,S,G,KQ,DL,H,R1,W,X,C1,Y,F,VS,VP,C2,AY,PJ
       1,BSV,BSA,PHI,DATA,PR,U,AVS,JNR,NEND,ALT,EL,Q,EZ,BSC,ELH,KASE,EM,EN
       1,N,ACC,RC,BONG,NV,NN,JOBS,WT,T,WL,VF,FL,APR,BVP,TEST,AF,HH
        S(7)=S(7)+DL
        IF(S(7)-Z(7,KEND)-5.)65,65,61
   65   DL=Z(7,KEND)+DL-S(7)
        S(7)=Z(7,KEND)
 61     DO 62 K=KQ,KEND
        IF(S(7)-Z(7,K))62,63,63
 62     CONTINUE
 63     KQ=K-1
        R=(S(7)-Z(7,KQ))/(Z(7,KQ+1)-Z(7,KQ))
        DO 64 J=1,6
 64     S(J)=Z(J,KQ)+R*(Z(J,KQ+1)-Z(J,KQ))
        RETURN
        END
```

```
*       LIST8
*       LABEL
*       SYMBOL TABLE
        SUBROUTINE LINT
        DIMENSION Z(9,100),S(9),W(9),X(9),Y(9),PJ(7),Q(9),AY(9),DATA(21,5,
       1 2),PHI(21)
        COMMON Z,KEND,CTH,STH,C,B,S,G,KQ,DL,H,R1,W,X,C1,Y,F,VS,VP,C2,AY,PJ
       1,BSV,BSA,PHI,DATA,PR,U,AVS,JNR,NEND,ALT,EL,Q,EZ,BSC,ELH,KASE,EM,EN
       1,N,ACC,RC,BONG,NV,NN,JOBS,WT,T,WL,VF,FL,APR,BVP,TEST,AF,HH
        DO 24 K=2,KQ
        EL=Z(3,K)/(C-Z(4,K))
        IF(ABSF(EL)-.999)20,21,21
   21   Q(1)=1.
        S(7)=Z(7,K)
        GO TO 23
   20   EN=-SQRTF(1.-EL*EL)
        X(4)=1./(Z(3,K)*EN)
        X(3)=Z(5,K)*X(4)
        X(2)=(FL*Z(3,K)+Z(4,K))*X(4)
        R2=SQRTF(1.+X(3)**2+X(2)**2)
        X(5)=C1*R2
         ZDL=Z(7,K)-Z(7,K-1)
         B=(Z(3,K)-Z(3,K-1))/ZDL
        BA=EL*(Z(4,K)-Z(4,K-1))/ZDL
   26   X(6)=-EL*(B+BA)/C/EN/H
         B=0.5*ZDL
         DO 22 M=2,6
        Y(M)=Y(M)+B*(W(M)+X(M))
 22     W(M)=X(M)
  25    F=(1.+Y(5)+Y(6))/H
        IF(F)27,27,29
   27   F=F-Y(5)/H
         Y(5)=0.
         W(5)=0.
         C1=0.0
         Q(2)=1.0
         Q(4)=Z(7,K)
   29   R4=R2/((Z(3,K)+Z(1,K))**2*SQRTF(F*Z(2,K)/Z(3,K))*Z(6,K))
        X(1)=(R1-R4)/SQRTF(Z(7,1)-Z(7,K))
         Y(1)=B*(W(1)+X(1))+Y(1)
         W(1)=X(1)
 24     CONTINUE
   23   RETURN
        END
```

```
*       LIST8
*       LABEL
*       SYMBOL TABLE
        SUBROUTINE FIN
        DIMENSION Z(9,100),S(9),W(9),X(9),Y(9),PJ(7),Q(9),AY(9),DATA(21,5,
       1 2),PHI(21)
        COMMON Z,KEND,CTH,STH,C,B,S,G,KQ,DL,H,R1,W,X,C1,Y,F,VS,VP,C2,AY,PJ
       1,BSV,BSA,PHI,DATA,PR,U,AVS,JNR,NEND,ALT,EL,Q,EZ,BSC,ELH,KASE,EM,EN
       1,N,ACC,RC,BONG,NV,NN,JOBS,WT,T,WL,VF,FL,APR,BVP,TEST,AF,HH
        Y(1)=Y(1)+2.*R1*SQRTF(Z(7,1)-S(7))
        EL=S(3)/(C-S(4))
        IF(ABSF(EL)-.999)26,27,27
   27   Q(1)=1.
        GO TO 30
   26   EN=-SQRTF(1.-EL*EL)
        X(4)=1./(EN*S(3))
        X(3)=S(5)*X(4)
        X(2)=(EL*S(3)+S(4))*X(4)
        R2=SQRTF(1.+X(2)**2+X(3)**2)
         ZDL=S(7)-Z(7,KQ)
         B=(S(3)-Z(3,KQ))/ZDL
        BA=EL*(S(4)-Z(4,KQ))/ZDL
        X(5)=C1*R2
   23   X(6)=-EL*(B+BA)/C/EN/H
         B=0.5*ZDL
         DO 25 M=2,6
        Y(M)=Y(M)+B*(X(M)+W(M))
 25     W(M)=X(M)
   24   F=(1.+Y(5)+Y(6))/H
         IF(F) 34,34,37
   34   F=F-Y(5)/H
        C1=0.
        Q(2)=1.
         Y(5)=0.0
         W(5)=0.0
         GO TO 37
   37   R4=R2/((S(3)+S(1))**2*S(6)*SQRTF(F*S(2)/S(3)))
        X(1)=(R1-R4)/SQRTF(Z(7,1)-S(7))
         Y(1)=B*(W(1)+X(1))+Y(1)
         W(1)=X(1)
        W(1)=W(1)-R1/SQRTF(Z(7,1)-S(7))
   28   DL=Z(7,KQ)
        KL=KEND-1
        DO 35 K=KQ,KL
        B=Z(7,K)-Z(7,K+1)
 35     DL=MIN1F(DL,B)
        DL=-.25*DL
   29   B=G*S(6)*S(3)*S(3)
        HA=SQRTF(Y(1)*S(2)*F*(Z(7,1)-S(7))/S(3))
        PR=C2/B/HA
         VS=S(3)*(1.+.4286*PR)
        VP=(VS-S(3))/DL
   33   F=F*(Z(7,1)-S(7))
   30   RETURN
        END
```

```
*       LIST8
*       LABEL
*       SYMBOL TABLE
        SUBROUTINE INTEG
        DIMENSION Z(9,100),S(9),W(9),X(9),Y(9),PJ(7),Q(9),AY(9),DATA(21,5,
       1 2),PHI(21)
        COMMON Z,KEND,CTH,STH,C,B,S,G,KQ,DL,H,R1,W,X,C1,Y,F,VS,VP,C2,AY,PJ
       1,BSV,BSA,PHI,DATA,PR,U,AVS,JNR,NEND,ALT,EL,Q,EZ,BSC,ELH,KASE,EM,EN
       1,N,ACC,RC,BONG,NV,NN,JOBS,WT,T,WL,VF,FL,APR,BVP,TEST,AF,HH
 41     EL=-VS/(S(4)-C)
        IF(ABSF(EL)-.999)415,43,43
   43 Q(1)=1.
        GO TO 49
 415    EN=-SQRTF(1.-EL*EL)
        X(4)=1./EN/VS
        X(2)=(EL*VS+S(4))*X(4)
        X(3)=S(5)*X(4)
        R2=SQRTF(1.+X(2)**2+X(3)**2)
        B1=(S(4)-U)*EL/DL
        X(5)=C1*R2
   44 X(6)=-EL*(VP+B1)/C/EN/H
         B=0.5*DL
         DO 42 M=2,6
 42     AY(M)=Y(M)+B*(W(M)+X(M))
        AF=1.+AY(5)+AY(6)
        IF(AF-.01)48,417,417
 48      AF=AF-AY(5)
        C1=0.
         AY(5)=0.0
         Y(5)=0.0
         W(5)=0.0
        Q(5)=3.
 417     F=(Z(7,1)-S(7))*AF/H
 416 X(1)=R2/S(6)/((S(3)+S(1))**2*SQRTF(S(2)*F/S(3)))
        X(1)=-X(1)
         AY(1)=Y(1)+B*(W(1)+X(1))
        B=G*S(6)*S(3)**2
        PR=.5*(C2/B/SQRTF(AY(1)*S(2)*F/S(3))+APR)
        VS=.5*(AVS+S(3)*(1.+.4286*PR))
         VP=(VS-AVS)/DL
   49 RETURN
        END
```

```
*       LABEL
*      SYMBOL TABLE
CSBOOM
      DIMENSION Z(9,100),S(9),W(9),X(9),Y(9),PJ(7),Q(9),AY(9),DATA(21,5,
     1 2),PHI(21)
      COMMON Z,KEND,CTH,STH,C,B,S,G,KQ,DL,H,R1,W,X,C1,Y,F,VS,VP,C2,AY,PJ
     1,BSV,BSA,PHI,DATA,PR,U,AVS,JNR,NEND,ALT,EL,Q,EZ,BSC,ELH,KASE,EM,EN
     1,N,ACC,RC,BONG,NV,NN,JOBS,WT,T,WL,VF,FL,APR,BVP,TEST,AF,HH
       COMMON CRV,PSI,TAU, PS,TS,XD,YD,ZD ,VT,MP
  310 READ 200,KEND,NEND,KASE,NV,NN,JOBS
      READ 201,(Z(7,K),Z(2,K),Z(1,K),Z(8,K),Z(9,K),K=1,KEND)
      READ 202,(PHI(N),N=1,NEND)
      READ 202,ACC,BONG,RC,EM,ALT,VF,FL,WT,T,WL,CRV,PSI,TAU
       UM=ASINF(1.0/EM) *57.2958
       IF (90.0-UM-PSI) 11,11,13
 11    PRINT 204,KASE,EM,ALT
       PRINT 218
 218   FORMAT (39HONO SHOCKS AT GROUND DUE TO CLIMB ANGLE)
       GO TO 38
 13   B=(ALT-100.*BONG)/1000.
      IF(B-Z(7,KEND))12,12,39
   12  PRINT 204, KASE,EM,ALT
      PRINT 213
      GO TO 38
   39 DO 112 K=1,KEND
      Z(7,K)=Z(7,K)*1000.
  112 Z(3,K)=49.*SQRTF(Z(1,K)+459.6)
    2 PRINT 205,KASE,EM,ALT,ACC,RC,VF,FL,WT,BONG,T,WL  ,PSI,TAU,CRV
      PRINT 206
       PRINT 207,(Z(7,K),Z(8,K),Z(9,K),Z(2,K),Z(3,K),Z(1,K),K=1,KEND)
       DVC=0.0
       MP=1
       IF (ABSF(PSI) + ABSF(CRV)) 40,40,41
 41    DVC=1.0
       CALL CORR
 40   CALL ALTA
 1    DO 111 N=1,NEND
      N=N
      DO 5 J=1,5
    5 DATA(N,J,MP)=0.
      CALL ONE
      S(7)=Z(7,1)-100.*BONG*COSF(PHI(N)/57.3)
C     ACOUSTIC INITIAL INTEGRATION
 14   KQ=1
      DL=0.
      CALL MID
      IF(KQ-1)18,18,19
 19   CALL LINT
      IF(Q(2)-1.)25,23,25
   23 Q(2)=0.
      PRINT 216,Q(4),PHI(N)
   25 IF(Q(1)-1.)18,21,18
 18   CALL FIN
      IF(Q(2)-1.)22,24,22
```

```
   24 Q(2)=0.
      PRINT 216,S(7),PHI(N)
   22 IF(Q(1)-1.)20,21,20
   21 PRINT 215,S(7),PHI(N)
      GO TO 111
C     SHOCK INTEGRATION STARTS HERE
   20 ADL=.75*DL
      DLT=DL
   80 U=S(4)
      AVS=VS
      BVP=VP
 81   CALL MID
   99 TEST=-2.
 85   CALL INTEG
   98 IF(Q(1)-1.)3,4,3
    4 Q(1)=0.
       IF (DL+10.0) 78,31,31
    3 IF(TEST+1.)82,83,83
   82 TEST=TEST+1.
      APR=PR
      GO TO 85
   83 V=2.*ABSF(PR-APR)/(PR+APR)
      IF(V-.01)86,86,87
   87 TEST=TEST+1.
      APR=PR
       IF(TEST-10.0) 85,85,88
   88 IF(DL+5.)78,77,77
   78 S(7)=S(7)-DL
      DL=.5*DL
   96 VS=AVS
      VP=BVP
      GO TO 81
 77    PRINT 217,PHI(N)
      GO TO 91
   31 PRINT 214,PHI(N)
   91 PRINT 211
      DATA(N,4,MP)=-1.0
      GO TO 90
   86 IF(NN-N)89,37,89
 37    IF (DVC-1.0) 45,45,89
 45    IF (EZ) 36,36,90
   36 EZ=1.
      PRINT 210,(PHI(NN))
      PRINT 211
   90 PJ(6)=S(2)
      PJ(4)=PR
      PJ(5)=S(2)*PR
      PJ(1)=S(7)
      PJ(3)=    AY(3)*CTH+AY(2)*STH+AY(4)*Z(9,1)
      PJ(2)=    AY(2)*CTH-AY(3)*STH+AY(4)*Z(8,1)
      PRINT 212,(PJ(I),I=1,6)
       IF (DATA(N,4,MP)) 111,89,89
 89    DO 71 M=1,6
      W(M)=X(M)
```

```
71    Y(M)=AY(M)
      IF(DL+10.)72,76,76
76     DL=ADL
  72 IF(S(7)-Z(7,KEND))70,70,95
95     IF (Q(5)-1.0) 92,93,94
92     IF (AF-0.05) 97,97,80
97     DL=MAX1F(-50.0,DL)
       GO TO 80
  94 Q(5)=Q(5)-1.
     GO TO 80
  93 DL=DLT
       Q(5)=0.0
     GO TO 80
70     DATA(N,1,MP)=RC*Z(2,KEND)*PR
       DATA(N,4 ,MP)=Y(4)
       DATA(N,3,MP)=Y(4)*Z(9,1)+Y(2)*STH+Y(3)*CTH
       DATA(N,2,MP)=Y(2)*CTH-Y(3)*STH+Y(4)*Z(8,1)
111  CONTINUE
       IF (DVC-1.0) 42,48,49
48     DVC=2.0
       ALT=ALT+ZD
       PSI=PSI-VT*CRV*SIGNF(TAU,PSI)
       MP=2
       GO TO 40
49     CALL SORT
       GO TO 38
42   VG=SQRTF(Z(9,1)**2+(EM*Z(3,1)-Z(8,1))**2)
     B=Z(9,1)/VG
     BB=(EM*Z(3,1)-Z(8,1))/VG
     DO 102 N=1,NEND
       IF (DATA(N,4,MP)) 101,101,103
101    DATA(N,2,MP)=0.
       DATA(N,3,MP)=0.
       DATA(N,1,MP)=0.
     GO TO 102
103    DST=VG*(DATA(N,4,MP)-DATA(NV,4,MP))
       DATA(N,2,MP)=DATA(N,2,MP)+DST*BB
       DATA(N,3,MP)=DATA(N,3,MP)-DST*B
 102 CONTINUE
       PRINT 204, KASE,EM,ALT
     PRINT 203
     PRINT 208
       PRINT 209,(PHI(N),(DATA(N,J,MP),J=1,4),N=1,NEND)
  38 IF(JOBS)311,310,310
 311 CALL EXIT
 200 FORMAT(6I10)
 201 FORMAT(F10.0,4F10.3)
 202 FORMAT(7F10.2)
 203 FORMAT(19H0SHOCK-GROUND DATA )
 204 FORMAT(18H1SONIC BOOM, CASE I5,5H,  M=F6.3,12H,  ALTITUDE=F7.0)
205  FORMAT(18H1SONIC BOOM, CASE I5,5H,  M=F6.3,12H,  ALTITUDE=F7.0,7H,
    1  ACC=F7.3,5H, RC=F4.2,5H, VF=F6.3,5H, LF=F6.3/1H ,5H  WT=F9.1,9H,
    1 LENGTH=F6.1,6H,  FR=F5.2,5H, WL=F6.3,8H, ANGLE=F7.2,6H, TAU=F6.2,
    1 4HSEC.12H, CURVATURE=F7.3/1H0)
```

```
206  FORMAT (1H08X8HALTITUDE7X8HHEADWIND8X8HSIDEWIND8X8HPRESSURE4X11HSO
    1UND SPEED4X11HTEMPERATURE/11X4H(FT)11X5H(FPS)11X5H(FPS)11X5H(PSF)8
    2X5H(FPS)9X7H(DEG F)/1H )
207  FORMAT (1H F15.0,3F16.3,F13.3,F15.3)
 208 FORMAT(1H0,9X,5HANGLE,/X,13HPRESSURE JUMP, 6X,1HX,15X,1HY,10X,4HTI
    1ME/1H ,9X,5H(DEG),10X,5H(PSF),9X,4H(FT),12X,4H(FT),9X,5H(SEC)/1H )
 209 FORMAT(1H ,F14.2,F15.3,2F15.0,F13.2)
 210 FORMAT(1H0,43HHISTORY OF SHOCK STRENGTH VARIATION, ANGLE= F6.2)
 211 FORMAT(1H0,11X,1HZ,15X,1HX,15X,1HY,8X,45HPRESSURE RATIO      PRESSU
    1RE JUMP      PRESSURE/1H , 9X,4H(FT),12X,4H(FT),12X,4H(FT),31X,5H(P
    1SF),10X,5H(PSF)/1H )
 212 FORMAT(1H ,3F15.0,F19.7,F17.3,F15.3)
 213 FORMAT(1H0,38HGROUND IS CLOSER THAN 100 BODY LENGTHS)
 214 FORMAT(24H0CUTOFF ALTITUDE, ANGLE=F6.2)
 215 FORMAT(42H0CUTOFF BEFORE 100 BODY LENGTHS, ALTITUDE=F10.2,8H, ANGL
    1E=F6.2)
 216 FORMAT(56H0ACCELERATION EFFECTS BEFORE 100 BODY LENGTHS, ALTITUDE=
    1F10.2,8H, ANGLE=F6.2)
217   FORMAT (38H0COMPUTATION DOES NOT CONVERGE, ANGLE=F6.2)
      END
```

```
*       LISTB
*       LABEL
*       SYMBOL TABLE
        SUBROUTINE CORR
      DIMENSION Z(9,100),S(9),W(9),X(9),Y(9),PJ(7),Q(9),AY(9),DATA(21,5,
     1 2),PHI(21)
      COMMON Z,KEND,CTH,STH,C,B,S,G,KQ,DL,H,R1,W,X,C1,Y,F,VS,VP,C2,AY,PJ
     1,BSV,BSA,PHI,DATA,PR,U,AVS,JNR,NEND,ALT,EL,Q,EZ,BSC,ELH,KASE,EM,EN
     1,N,ACC,RC,BONG,NV,NN,JOBS,WT,T,WL,VF,FL,APR,BVP,TEST,AF,HH
        COMMON CRV,PSI,TAU, PS,TS,XD,YD,ZD ,VT,MP
        VALF(X)=SQRTF(1.0+(ALF+2.0*BETA*X)**2)
        CRV=CRV*1.0E-06
        PSI=PSI/57.2957795
        IF (PSI) 3,4,3
 4      PSI=ABSF(PSI)
 3      TS=SIGNF(TAU,PSI)
        VT=SQRTF(((EM*Z(3,1))*COSF(PSI)-Z(8,1))**2+((EM*Z(3,1))*SINF(PSI)
     1)**2)
        ALF=-TANF(PSI)
        BETA=0.5*CRV*(1.0+ALF**2)**1.5
        XD=0.
        QUAD=0.
        DO 1 I=1,10
        IF (XD) 11,12,11
 11     QUAD=(VALF(0.)+4.0*VALF(XD/2.0)+VALF(XD))*XD/6.0
 12     XI=XD
        XD=XI-(QUAD-TS*VT)/VALF(XI)
        IF(ABSF((XD-XI)/XD)-0.01) 2,2,1
 1      CONTINUE
        PRINT 1100,XI,XD
 1100   FORMAT (1H014HERROR MESSAGE.2X53HX CORRECTION FOR CURVED FLIGHT P
     1ATH DID NOT CONVERGE./1H0)
 2      ZD=(XD*BETA+ALF)*XD
        YD=-TS*Z(9,1)
        IF (ZD) 5,5,44
 44     IF (PSI) 45,46,45
 45     XD=-XD
        YD=-YD
        ZD=-ZD
        PSI = PSI-VT*CRV*TS
        GO TO 5
 46     PSI=  TAU*VT*CRV
       ZD=-ZD
 5      PSI=PSI*57.2957795
        RETURN
        END
```

```
*       LIST8
*       LABEL
*       SYMBOL TABLE
        SUBROUTINE SORT
      DIMENSION Z(9,100),S(9),W(9),X(9),Y(9),PJ(7),Q(9),AY(9),DATA(21,5,
     1 2),PHI(21) ,J(21) ,SG(21,5)
      COMMON Z,KEND,CTH,STH,C,B,S,G,KQ,DL,H,R1,W,X,C1,Y,F,VS,VP,C2,AY,PJ
     1,BSV,BSA,PHI,DATA,PR,U,AVS,JNR,NEND,ALT,EL,Q,EZ,BSC,ELH,KASE,EM,EN
     1,N,ACC,RC,BONG,NV,NN,JOBS,WT,T,WL,VF,FL,APR,BVP,TEST,AF,HH
        COMMON CRV,PSI,TAU, PS,TS,XD,YD,ZD ,VT,MP
        NSUM=2*NEND
        TAVG=0.
        DO 100 N=1,NEND
        J(N)=2
        IF(DATA(N,4,2))11,11,12
 11     DO 110 L=1,3
 110    DATA(N,L,2)=0.
        J(N)=1
        GO TO 10
 12     DATA(N,4,2)=DATA(N,4,2)-TS
        DATA(N,3,2)=DATA(N,3,2)+YD
        DATA(N,2,2)=DATA(N,2,2)+XD
 10     IF (DATA(N,4,1))13,13,14
 13     DO 130 L=1,3
 130    DATA(N,L,1)=0.
        J(N)=1
 14     IND=J(N)
        GO TO (15,16),IND
 15     NSUM=NSUM-2
        GO TO 100
 16     TAVG=TAVG+DATA(N,4,1)+DATA(N,4,2)
 100    CONTINUE
        IF (NSUM) 17,17,18
 17     K=1
        GO TO 300
 18     K=2
        TAVG=TAVG/FLOATF(NSUM)
        DO 200 N=1,NEND
        IND=J(N)
        GO TO (21,22),IND
 21     DO 210 L=1,3
 210    SG(N,L)=0.0
        GO TO 200
 22     B=(DATA(N,4,1)-TAVG)/(DATA(N,4,1)-DATA(N,4,2))
        DO 220 L=1,3
 220    SG(N,L)=DATA(N,L,1)-B*(DATA(N,L,1)-DATA(N,L,2))
 200    CONTINUE
 300    PRINT 1100,KASE,EM
 1100 FORMAT(18H1SONIC BOOM, CASE I5,5H,  M=F6.3/
     1        1H0,9X,5HANGLE,7X,13HPRESSURE JUMP, 6X,1HX,15X,1HY,10X,4HTI
     1ME/1H ,9X,5H(DEG),10X,5H(PSF),9X,4H(FT),12X,4H(FT),9X,5H(SEC)/1H0
     1 18H  RAY-GROUND DATA )
        ALTI=ALT-ZD
        PRINT 1101,ALTI,(PHI(N),(DATA(N,L,1),L=1,4),N=1,NEND)
        PRINT 1101,ALT ,(PHI(N),(DATA(N,L,2),L=1,4),N=1,NEND)
 1101   FORMAT (12H0ALTITUDE = F7.0/(F15.2,F15.3,2F15.0,F13.2))
        PRINT 1102
 1102   FORMAT (1H0/19H0SHOCK-GROUND DATA /1H0)
        GO TO (301,302),K
 301    PRINT 1103
 1103   FORMAT (1H021HNO SHOCK-GROUND DATA.)
        RETURN
 302    PRINT 1104,(PHI(N),(SG(N,L),L=1,3),TAVG,N=1,NEND)
 1104   FORMAT (F15.2,F15.3,2F15.0,F13.2)
        RETURN
        END
```

APPENDIX IV

CLIMBING, DIVING, AND FLIGHT PATH CURVATURE EFFECTS

AIV.1 RAY ANGLE GEOMETRY

In this section we will describe an extension to the general theory which is given in Ref. 1. This extension will permit inclusion of flight paths which are curved, climbing, or diving. The results, however, are restricted to aircraft motions which are in a vertical plane. The contributions which arise from lateral motions can be determined by going through geometrical arguments very similar to those given below.

To include diving and climbing effects in the general theory we first introduce a new coordinate system (x^*, y^*, z^*).

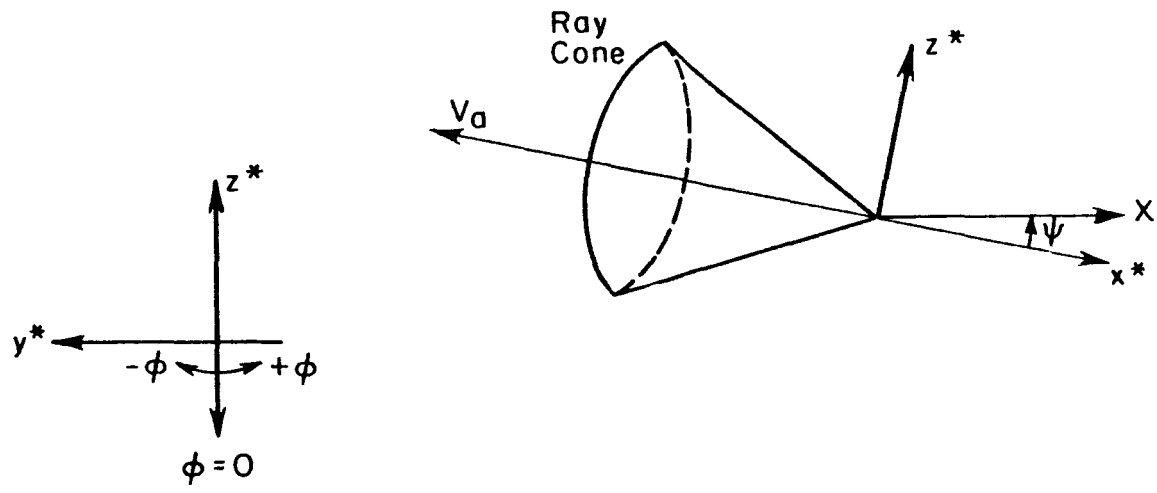

Figure AIV.1

x^* is tangent to the flight path and the velocity is in the negative x^* direction, y^* is perpendicular to x^* and is horizontal, z^* is perpendicular to y^* and x^* and points upward. The coordinates (x^*, y^*, z^*) are to form a right-handed system, and the aircraft is moving in the x^*, z^* plane. The angle ϕ will be used to identify any ray in the initial ray cone (see Fig.AIV.1) This angle has the same meaning as that defined in Fig. II.1, page 5 and Fig. 1, Ref. 1. Any unit vector in the initial ray cone (which is normal to the initial shock cone) has components relative to x^*, y^*, z^*, given in

terms of Mach angle and rotation angle ϕ:

$$\left.\begin{aligned} N_{x*} &= -\sin\mu \\ N_{y*} &= -\cos\mu\,\sin\phi \\ N_{z*} &= -\cos\mu\,\cos\phi \end{aligned}\right\} \qquad \text{(A IV.1)}$$

For climbing aircraft the angle ψ, between $x*$ and (horizontal) X is positive; for diving aircraft ψ is negative. That is, ψ is measured from the $x*$ to the X axes, positive in the counterclockwise direction. The components of unit vector N, given in (A IV.1), relative to X, Y, Z coordinates are

$$\left.\begin{aligned} N_X &= -\sin\mu\,\cos\psi - \cos\mu\,\cos\phi\,\sin\psi \\ N_Y &= -\cos\mu\,\sin\phi \\ N_Z &= \sin\mu\,\sin\psi - \cos\mu\,\cos\phi\,\cos\psi \end{aligned}\right\} \qquad \text{(A IV.2)}$$

We now want to construct the "ray coordinate system" x, y, z. Recalling (see discussion below Eq. (A.11) of Ref. 1) that the angle θ is determined by requiring the ray to be initially in the x, y, z plane; we let ℓ, m, n be the x, y, z direction cosines of the unit vector N.

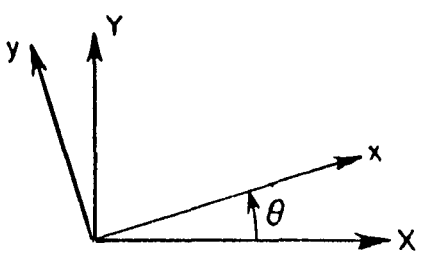

Rotating about the Z = z axis:

$$\left.\begin{aligned} \ell &= N_X\cos\theta + N_Y\sin\theta \\ m &= -N_X\sin\theta + N_Y\cos\theta \\ n &= N_Z \end{aligned}\right\} \qquad \text{(A IV.3)}$$

In order to have m = 0:

$$\left.\begin{aligned} \tan\theta &= \frac{N_y}{N_x} = \frac{\cos\mu \sin\phi}{\sin\mu \cos\psi + \cos\mu \cos\phi \sin\psi} \\ \sin\theta &= \frac{-N_y}{\sqrt{N_y^2 + N_x^2}}, \quad \cos\theta = \frac{-N_x}{\sqrt{N_y^2 + N_x^2}} \end{aligned}\right\} \quad \text{(A IV.4)}$$

Combining the results of Eqs. (A IV.3) and (A IV.4), the initial x direction cosine of the ray is

$$\ell_h = -\cos\mu \sqrt{\left[\tan\mu \cos\psi + \cos\phi \sin\psi\right]^2 + \sin^2\phi} \qquad \text{(A IV.5)}$$

Eqs. (A IV.4) and (A IV.5) reduce to Eqs. (3.3) and (3.4) of Ref. 1 when the climb or dive angle ψ equals zero. Also, all the results of Ref. 1 can be applied using the more general definitions given in (AIV.4) and (AIV.5).

The results presented in this section make it possible to determine the ray locations and shock strengths for aircraft on straight climbing or diving flight paths. However the technique used for determining the shock-ground intersection curve (see page 15) is inapplicable to the diving-climbing aircraft problem. This is because for each instant along the flight path, the rays leaving the aircraft will have a different ground intersection curve. The main reason for this is that the aircraft altitude is continuously changing. The technique developed on page 15 assumes that each set of ray-ground intersections is the same and to know any one implies knowledge of all, therefore a shock-ground curve can be constructed although the rays that meet it have left the aircraft at different times. In the third section of this appendix we will describe a method for determining an approximate shock-ground intersection.

It is not too difficult to include aircraft flight path curvature in the analysis. This is of considerable importance for determining the ray tube area used in shock strength computations. If the flight path is concave downward, two successive rays will be directed toward each other in a manner very similar to that of an accelerating aircraft. At some point below the aircraft the rays will converge leading, locally, to a high shock overpressure. The theory for this will be derived in the next section.

AIV.2 FLIGHT PATH CURVATURE

In Section IV.2, page 25, perturbations to the ray inclination angle, ν, were found. These perturbations arise from two effects; the first, $\Delta_1 \nu$, is the initial difference in the slopes of two successive rays due to aircraft acceleration. If the aircraft were flying on a curved flight path there would be an additional contribution to the difference $\Delta_1 \nu$. We will derive this second contribution in this section.

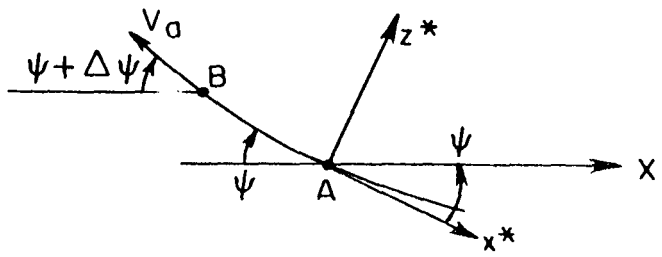

At the initial point, A, the flight path is at an angle ψ with respect to the horizontal; at point B (assumed to be an infinitesimal distance from A) the angle has changed to $\psi + \Delta\psi$. Relative to a coordinate system setup at B, the components of a unit vector, identified by the angle $\overline{\phi}$, in the ray cone has components (see Eq. (AIV.1).

$$\left.\begin{aligned} \overline{N}_{\overline{x}} &= -\sin\mu \\ \overline{N}_{\overline{y}} &= -\cos\mu \sin\overline{\phi} \\ \overline{N}_{\overline{z}} &= -\cos\mu \cos\overline{\phi} \end{aligned}\right\} \qquad \text{(AIV.6)}$$

The bar notation is used to indicate variables at point B. In order to relate the components of $\overline{N}$ in (A IV.6) to the x^*, y^*, z^* system we must rotate an amount $\Delta\psi$ about the y axis. Keeping terms of first order in $\Delta\psi$; i.e., $\sin \Delta\psi$, $\cos \Delta\psi = 1$

$$\left.\begin{aligned} \overline{N}_{x^*} &= -\sin\mu - \cos\mu \cos\overline{\phi}\, \Delta\psi \\ \overline{N}_{y^*} &= -\cos\mu \sin\overline{\phi} \\ \overline{N}_{z^*} &= \sin\mu\, \Delta\psi - \cos\mu \cos\overline{\phi} \end{aligned}\right\} \qquad \text{(A IV.7)}$$

We now must identify the angle $\overline{\phi}$ with the angle ϕ used in the previous section. At point A, we passed a plane through the x^* axis making an angle ϕ with the vertical (see Fig. A IV.1). At point B we passed a plane through the $\overline{x}$ axis making an angle $\overline{\phi}$ with the vertical. In order that the two rays, corresponding to ϕ at A and $\overline{\phi}$ at B, lie in the same plane, defined by ϕ, we must have

$$\frac{N_{y^*}}{N_{z^*}} = \tan\phi = \frac{\cos\mu \sin\overline{\phi}}{\cos\mu \cos\overline{\phi} - \sin\mu\, \Delta\psi} \quad . \qquad \text{(A IV.8)}$$

Letting $\overline{\phi} = \phi + \Delta\phi$ we obtain from (A IV.8)

$$\Delta\phi = -\sin\phi \tan\mu\, \Delta\psi \qquad \text{(A IV.9)}$$

We can now determine the change in initial ray direction due to changes in both aircraft Mach number and flight path slope. First we recall the identity

$$\sin\nu = -\ell$$

therefore

$$\Delta_1 \nu = -\sec\nu_h\, \Delta\ell_h \, . \qquad \text{(A IV.10)}$$

By using (A IV.5) we can determine

$$\left.\begin{aligned} \Delta \ell_h &= \frac{\partial \ell_h}{\partial \mu} \frac{d\mu}{dM} \Delta M + \frac{\partial \ell_h}{\partial \psi} \Delta\psi \\ \text{where } \sin\mu &= 1/M, \quad \frac{d\mu}{dM} = -\left(M\sqrt{M^2-1}\right)^{-1}, \quad \Delta M = \frac{\Delta V_a}{a_h} \end{aligned}\right\} \quad \text{(A IV.11)}$$

After carrying out the differentiations in (A IV.11), using (A IV.9), and substituting the result in A IV.10) we obtain, finally:

$$\Delta_1 \nu = -\sec \nu_h \left[\frac{\Delta v_a \cos^2 \nu_h}{M(M^2-1)a_h \,|\, \ell_h \,|} \left\{ 1 - \frac{\sin\psi}{\cos^2 \nu_h} \left(\sin\psi - \cos\phi\cos\psi\sqrt{M^2-1}\right) \right\} \right.$$

$$\left. - \frac{\Delta\psi \cos\phi}{M} \left\{ \cos\theta \left(\cos\psi\sqrt{M^2-1} - \sin\psi\cos\phi\right) - \sin\theta\sin\phi \right\} \right]$$

(A IV.12)

It is easily shown that for a straight and level flight, $\psi = \Delta\psi = 0$, Eq. (A IV.12) reduces to Eq. (IV.9) on page 26. Of the terms multiplying $\Delta\psi$, the one $\cos\theta\cos\psi\sqrt{M^2-1}$ is largest. Therefore the coefficient of $\Delta\psi$ is positive and a negative curvature, $\Delta\psi < 0$, has the same effect as a positive acceleration. For an accelerating, climbing (take off) flight path the effects of a positive acceleration and curvature will offset each other. Similarly for a decelerating, diving (landing) flight path the negative acceleration and curvature offset each other.

With $\Delta_1 \nu$ given in (A IV.12) the ray tube area term (see Eqs.(IV.12)

and (III.2)) is

$$A = z \sec \nu_h \left[1 - s \left\{ \frac{\dot{V}_a \left[M^2 (M^2 - 1) \right]^{-1}}{a_h^2 \, | \ell_h | \cos \theta} \left(1 - \frac{\sin \psi}{\cos^2 \nu_h} \left[\sin \psi - \cos \psi \cos \phi \sqrt{M^2 - 1} \right] \right) \right.\right.$$

$$\left.\left. - k \frac{\cos \phi}{M \cos^2 \nu_h} \left(\cos \psi \sqrt{M^2 - 1} - \sin \psi \cos \phi - \tan \theta \sin \phi \right) \right\}\right.$$

$$\left. + \frac{\sec \nu_h}{V_a \cos \theta} \int_h^z \tan \nu \left(\frac{dV_s}{dz} - \sin \nu \frac{du_0}{dz} \right) dz \right] \qquad \text{(A IV.13)}$$

The term k is the rate of change of flight path angle with respect to distance along the flight path

$$\text{i.e., } k = \frac{1}{V_a} \frac{d\psi}{dt}$$

This is, by definition, the flight path curvature.

The curvature can be related to aircraft motions as follows: Consider a curved flight path,

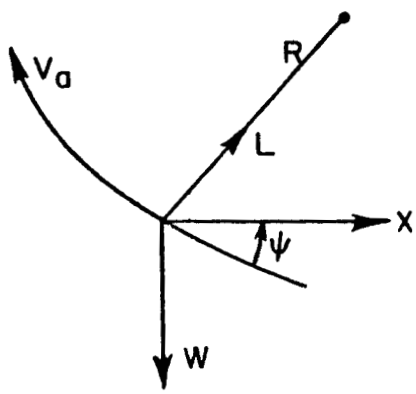

L = lift

W = weight

R = radius of curvature

Figure A IV.2

with the (simplified) force diagram as shown in Fig. A IV. 3. Balancing the radial forces at the instantaneous center of curvature

$$\frac{W}{g} \frac{V_a^2}{R} = L - W \cos \psi$$

$$\text{therefore } k = \frac{1}{R} = \frac{(L - W \cos \psi) g}{W V_a^2}$$

When lift, L, is greater than W cos ψ the aircraft is increasing its flight path angle and the curvature is positive; when L is smaller than W cos ψ the curvature is negative.

A IV.3 SHOCK GROUND INTERSECTION

When an aircraft is either climbing or diving the shock-ground intersection curve varies with time. The problem is, therefore, basically different from the one in which the aircraft is flying horizontally. This latter problem is truly a steady state situation and the shock-ground intersection curve is invariant.

The shock-ground curve is the locus of disturbances which reach the ground simultaneously. By integrating the ray equations (III.1) we obtain the locus of disturbances which leave the aircraft at the same time. There are many ways to determine a shock curve when ray curve data are known; however the one chosen, and described below, seems to be comparatively simple and uses a minimum of computer time.

Two points on the flight path are determined which are separated, in time, by an increment τ. Then, the ray ground intersections are computed for each of these points. To be specific, assume data are determined for seven angles ϕ about the flight path; therefore the computer determines seven ray-ground X, Y coordinates, seven ray travel times, and seven pressure jumps for each of the two points on the flight path. A mean ray travel time is then found by simply averaging the fourteen computed travel times; i.e.,

$$t_{mean} = \frac{1}{14} \sum_{i=1}^{7} (t_{Ai} + t_{Bi}) \qquad \text{(A IV. 14)}$$

where t_{Ai} or t_{Bi} is the ray travel time from point A or B on the flight path corresponding to angle ϕ_i . Then, using this mean time, we determine by linear interpolation (or extrapolation) the corresponding X, Y coordinates and the pressure jump Δp as follows:

$$X_{i\ mean} = X_{Ai} + \frac{t_{Ai} - t_{mean}}{t_{Ai} - t_{Bi}} (X_{Bi} - X_{Ai}) \qquad \text{(A IV.15)}$$

with the identical formula being used with Y or Δp substituted for X.

The resulting coordinates are, approximately, the ground intersection points of disturbances (shock) arriving at the ground simultaneously. The pressure jumps are the pressure jumps across this shock.

It is recognized that the above computation gives some hypothetical "mean" shock and its strength. This is simply intended as an aid in visualizing the ground-shock pattern. The computer will print out the ray-ground data for both flight path points as well as the derived shock data, and the operator can interpret all the data as he so desires.

A IV.4 PROGRAM DETAILS

Program Inputs

The last three entries on the "aircraft data cards" (see page 6) are the flight path curvature (1/ft), the climb or dive angle (deg), and the time increment τ (sec) between the two flight path points. Since the curvature is usually a very small number it is to be read in as (curvature) x 10^6. A positive curvature indicates the flight path angle is increasing, and a negative curvature indicates a decreasing flight path angle. A climbing aircraft will have a positive flight path angle, and a diving aircraft a negative angle. The time increment between flight path points has been left as an input for the convenience of the operator. It has been found that a five-second interval has led to satisfactory results.

Program Calculations

If both the curvature and the climb (or dive) angle are zero the SBCP will operate as described in the main body of this report. If either one or both are nonzero two additional subroutines are used. These are named CORR and SORT. These will be described below.

SUBROUTINE CORR - In this subroutine the second point on the flight path is determined, assuming that the first point is at the origin. Since motion in the vertical X, Z plane the flight path can be approximately described as

$$\left.\begin{aligned} z &= \alpha x + \beta x^2 \\ \text{with} \quad \alpha &= -\tan \psi, \ \beta = 1/2\, k\, (1 + \alpha^2)^{3/2} \\ \psi &= \text{flight path angle (see Fig. A IV.1)} \\ k &= \text{flight path curvature} \end{aligned}\right\} \qquad \text{(A IV.16)}$$

If the aircraft flight path velocity (see Fig. A IV.3) relative to a fixed coordinate system were denoted V_T, we can write

$$V_T = \sqrt{\dot{x}^2 + \dot{z}^2} = -\frac{dx}{dt} \sqrt{1 + (\alpha + 2\beta x)^2} \qquad \text{(A IV.17)}$$

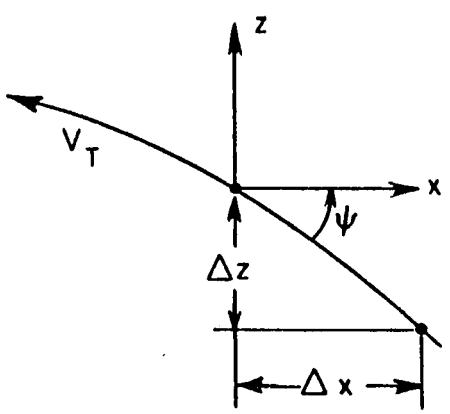

Figure A IV. 3

Integrating (A IV.17) over the time increment τ, assuming V_T is constant

$$\tau V_T + \int_0^{\Delta x} \sqrt{1 + (\alpha + 2\beta x)^2}\, dx = 0 \qquad \text{(A IV.18)}$$

solution of (A IV.18) for Δx gives the x coordinate of the second point on the flight path, this is accomplished in subroutine CORR by a Newton-Raphson iteration. Equation (A IV.16) is then used to determine Δz. In subroutine ALTA all atmospheric data above the flight altitude are discarded. This means that whenever two points on the flight path are used the higher one must be computed first. Subroutine CORR takes care of all situations for diving, climbing or level flight.

SUBROUTINE SORT - In this subroutine the computed ray-ground data, for the two flightpath points, are referred to a common origin and time scale. The linear interpolation described in Eqs. (A IV.14 and 15) is then carried out, and finally all the data is printed.

APPENDIX V

EXPERIMENTAL RESULTS

In this section the results of several computations with the SBCP will be presented. For all the cases described the same aircraft model was used. Different flight and atmospheric conditions were investigated. The necessary aircraft parameters were:

weight	= 100,000 lbs.	volume factor	= .64
length	= 100 ft.	lift factor	= .6
max dia.	= 12 ft.		

The basic atmosphere, unless otherwise indicated, was taken from ARDC 1959 Model Atmosphere.

Figure A V.1

This figure indicates the ground-shock intersection curve for an aircraft flying above a jet stream.. Superimposed on the ARDC atmosphere the jet stream starts at 50,000 ft., builds up linearly to 200 ft/sec at 35,000 ft and then falls to zero again at 20,000 ft.

Five cases were tested. These were aircraft velocity 0° (parallel), 45°, 90° (cross jet), 135°, 180° (anti-parallel) to the jet stream direction. For all cases, effects on pressure jump across the shock were negligible by time the shock reached the ground. While propagating through the jet stream the shock strength ($\Delta p/p$) tends to increase when in a region where the headwind (tailwind) is increasing (decreasing); conversely shock strength tends to decrease when the headwind (tailwind) is decreasing (increasing). For all cases the variation within the jet stream was at most 10% from the uniform atmosphere case.

The three cases shown in Fig. AV.1 are uniform (no jet stream) atmosphere solid line; 45° jet stream, dash dot line; 90° (cross wind) dashed line. The groups of symbols correspond, reading from left to right, to ϕ angles 45°, 30°, 15°, 0°, −15°, −30° −45°. To facilitate identification the alternate angle symbols (45°, 15°, −15°, −45°) are filled in. It is interesting to note that the −45° ray for the 45° direction

jet stream gets cut off and never reaches ground. The $-45°$ ray, cross-wind case nearly gets cut off; it does get to the ground but considerably further out than the uniform atmosphere case.

Figure AV.2

For this case a perturbation on the ARDC temperature profile was introduced. A sample perturbation is shown in the left figure. Four cases are shown in the right figure.

1. standard atmosphere
2. temperature inversion and return to standard, centered at 10,000 ft.
3. temperature inversion and return to standard, centered at 5,000 ft.
4. temperature inversion between 5,000 ft. and ground.

In case (4) the temperature fell from standard at 5,000 ft. to about 25° F at the ground. For all cases the pressure jump decreases (increases) when the shock propagates into an increasing (decreasing)temperature region.

It should be noted that for a standard atmosphere the shock strength, Δp, remains nearly constant for almost all of its travel near the ground. See, for example, case (1). The reason for this is that although the pressure ratio $\Delta p/p$ is decreasing with distance in accordance with Whitham's theory, the ambient pressure, p, is increasing as the ground is approached. These two effects counterbalance each other and Δp remains nearly unchanged.

A further comment can be made. Almost all atmospheric perturbations which occur above about 15,000 ft. altitude are "forgotten" by time the shock reaches the ground. That is, it is only those phenomena occurring near the ground which will affect the shock strength at the ground.

Figure AV.3

Acceleration effects at different Mach numbers are investigated here. The Mach number has a pronounced effect on the location of the high pressure, due to focusing, region. Due to limitations of the ray tube approach the magnitude of the pressure jump at its peak value may

not be too accurate, however the location is correct. For all cases shown the shock directly below the aircraft is considered.

The pressure drops off considerably, after the high pressure peak. Also the pressure jump at the ground, for the M = 1.2 case for example is close to that which would occur for a nonaccelerating aircraft at the same initial flight condition. For the M = 1.1 case the shock is cut off before it reaches the ground, due to the increasing temperature as the ground is approached. For the M = 1.3 case the shock gets to the ground before the pressure peak is reached.

Note that the buildup to the pressure peak takes place over an extended region, approximately 10,000 ft for the M = 1.2 case. Whereas the actual, unusually high pressure region is quite localized.

Figure AV.4

For this case we considered the effect of a temperature inversion and acceleration induced pressure peaks near the ground. Conditions were setup so that for a standard atmosphere the pressure peak occurs at about 1000 ft altitude.

A temperature profile was introduced which was standard to 5,000 ft and then fell to 24°F at the ground. The effect of the inversion was to cause the pressure peak to occur sooner, i.e., at a higher altitude. The location of the pressure peak had, within the limitations of the present theory, very little effect on its magnitude.

Figure AV.5

This case was essentially the same as that shown in Figure AV.4 except that the aircraft altitude was 50,000 ft. For a standard atmosphere the shock meets the ground before the pressure peak occurs. However, when a temperature inversion, near the ground, is inserted the pressure peak occurs sooner; i.e., above the ground. The boom at the ground for this latter case, is actually less than that for the standard atmosphere plus acceleration case. If the ground altitude were about 2,000 ft. the boom in the presence of a temperature inversion could be much greater than the standard atmosphere case.

Figure AV.6

In this figure the effects of flight path curvature and aircraft acceleration are shown. A hypothetical (nonrealistic) situation was constructed to indicate the general shock behavior. The atmosphere was assumed to be constant with a sound speed equal to about 1000 ft/sec. This same atmosphere was used for problem on p. 42. In addition, an aircraft dive angle of 15 degrees was assumed.

The output for case 1 of Fig. AV.6 is given on the page following this figure. This output is typical of one for problems which include diving or climbing aircraft on curved flight paths as described in Appendix IV. Also, this output can be compared with the one on page 42 to see the difference in the ground effects between a horizontal flight and a diving flight. For the case on page 42 the pressure jump at the ground is lower although the aircraft Mach number was higher. This is due to the fact that for a diving aircraft the shock travel distance is less.

In case 1 of Figure AV.6 no acceleration or curvature effects were introduced. For case 2 an acceleration of 36.4 ft/sec^2 was used. For case 3 a flight path curvature of -14.5×10^{-6} ft.$^{-1}$ was chosen to cause a pressure peak at approximately the same altitude as for case 2. Case 4 shows the additive nature of these two effects, half the acceleration and half the curvature were used. For case 5 a positive curvature was introduced, this just cancelled the acceleration effects.

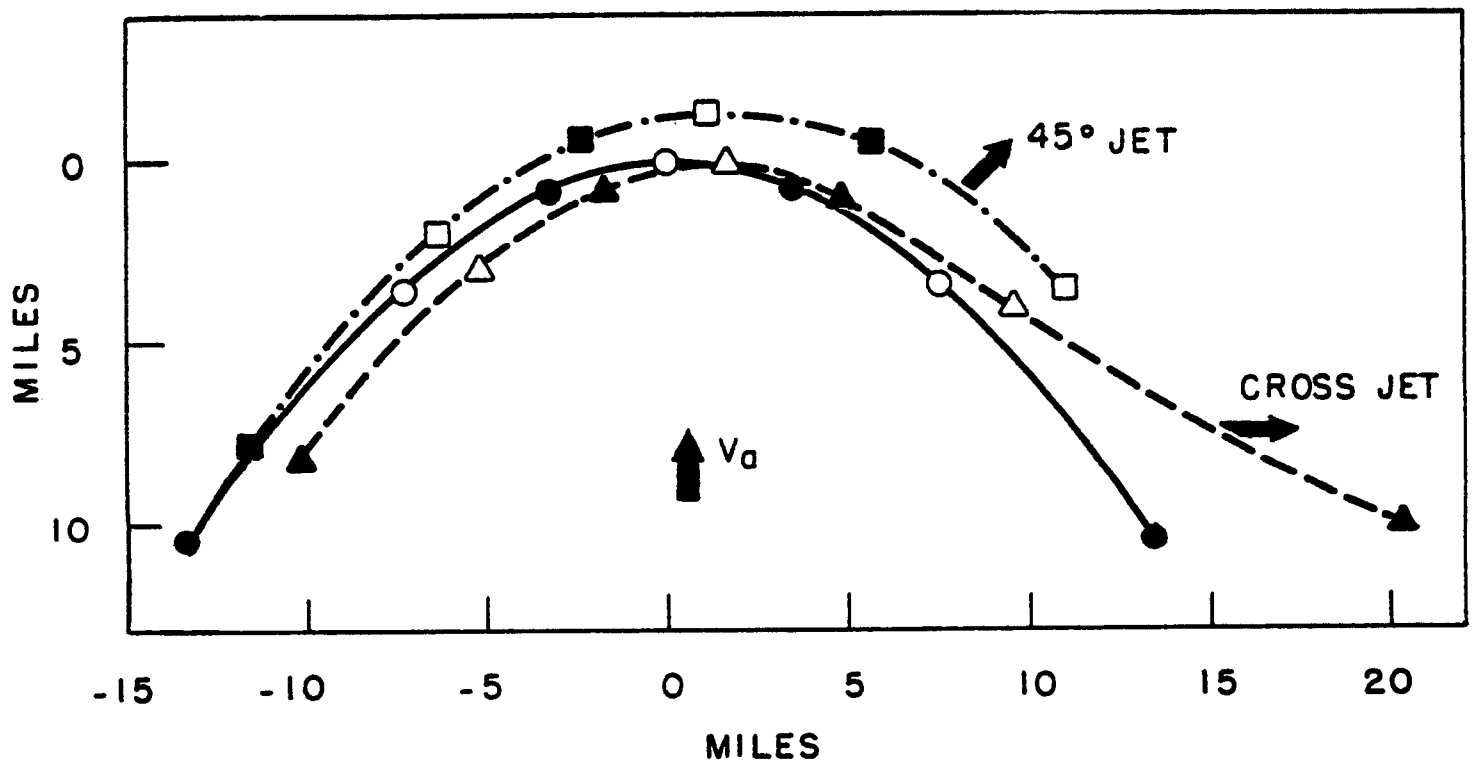

Figure AV.1. Shock-ground curves, M = 2, alt. = 60,000 ft, jet stream at 35,000 ± 15,000 ft.

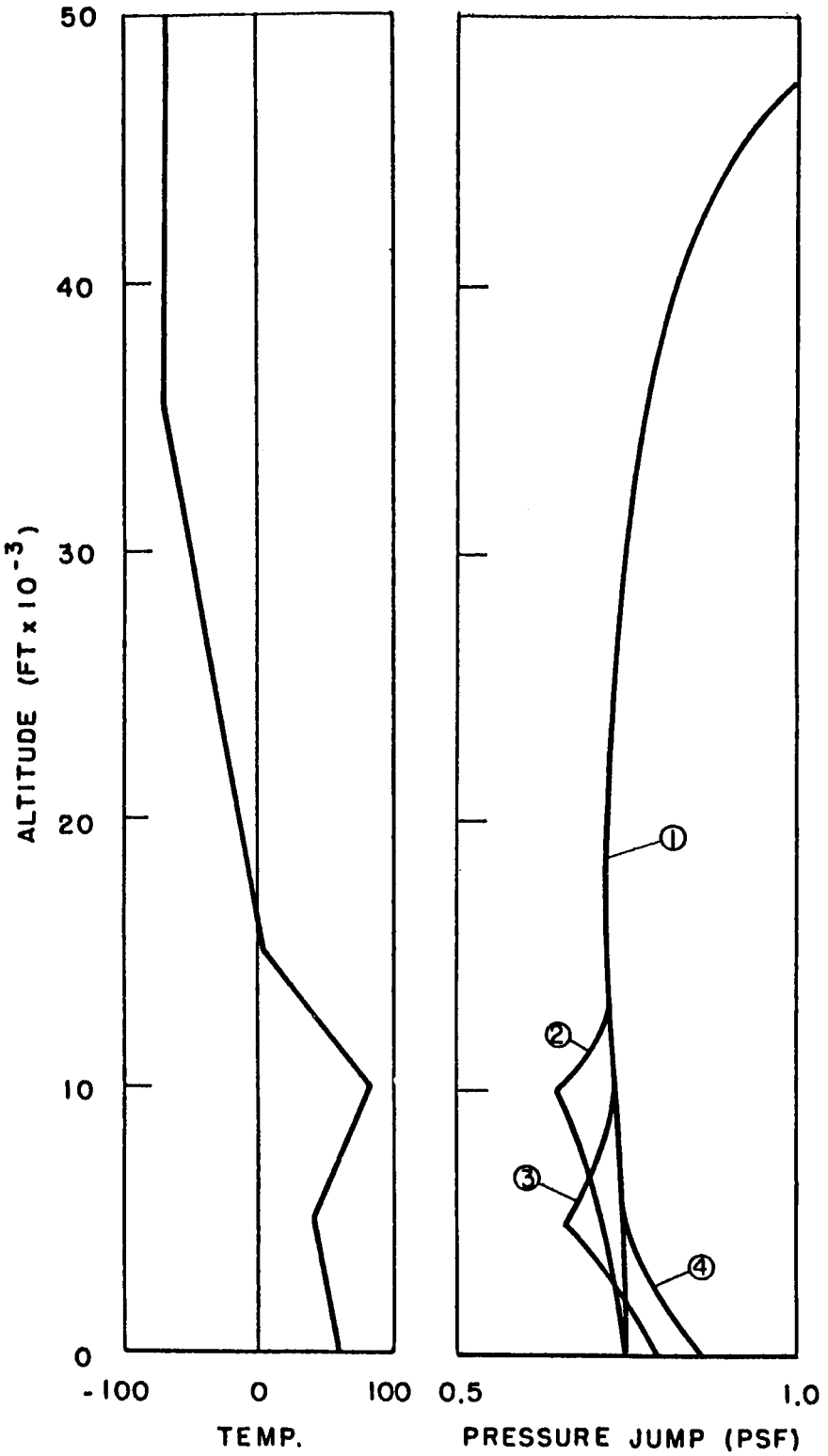

Figure AV.2. Temperature inversion, M = 2, alt. = 60,000 ft.

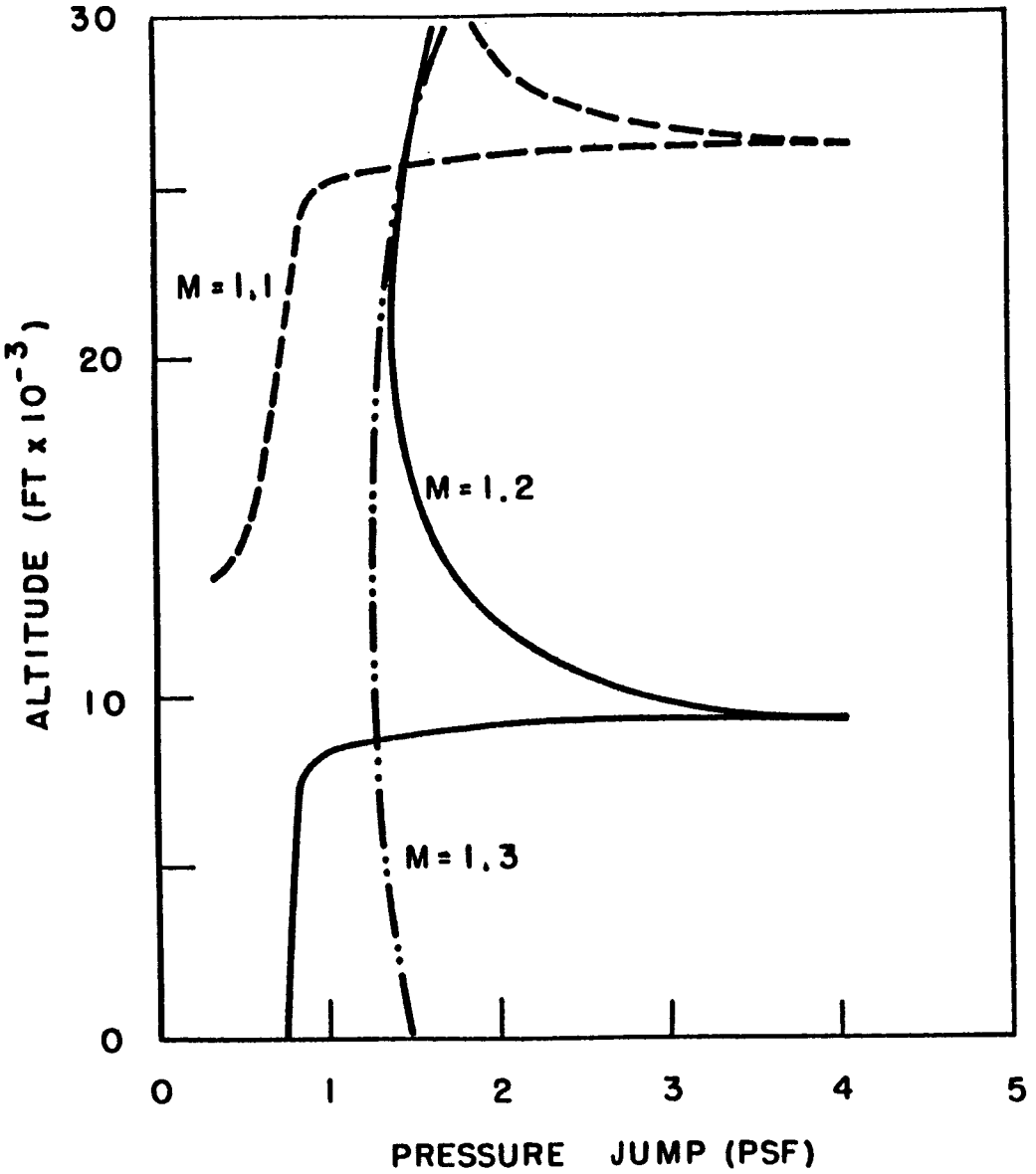

Figure AV.3. Acc'l. aircraft, st'd atmos., alt. = 40,000 ft.

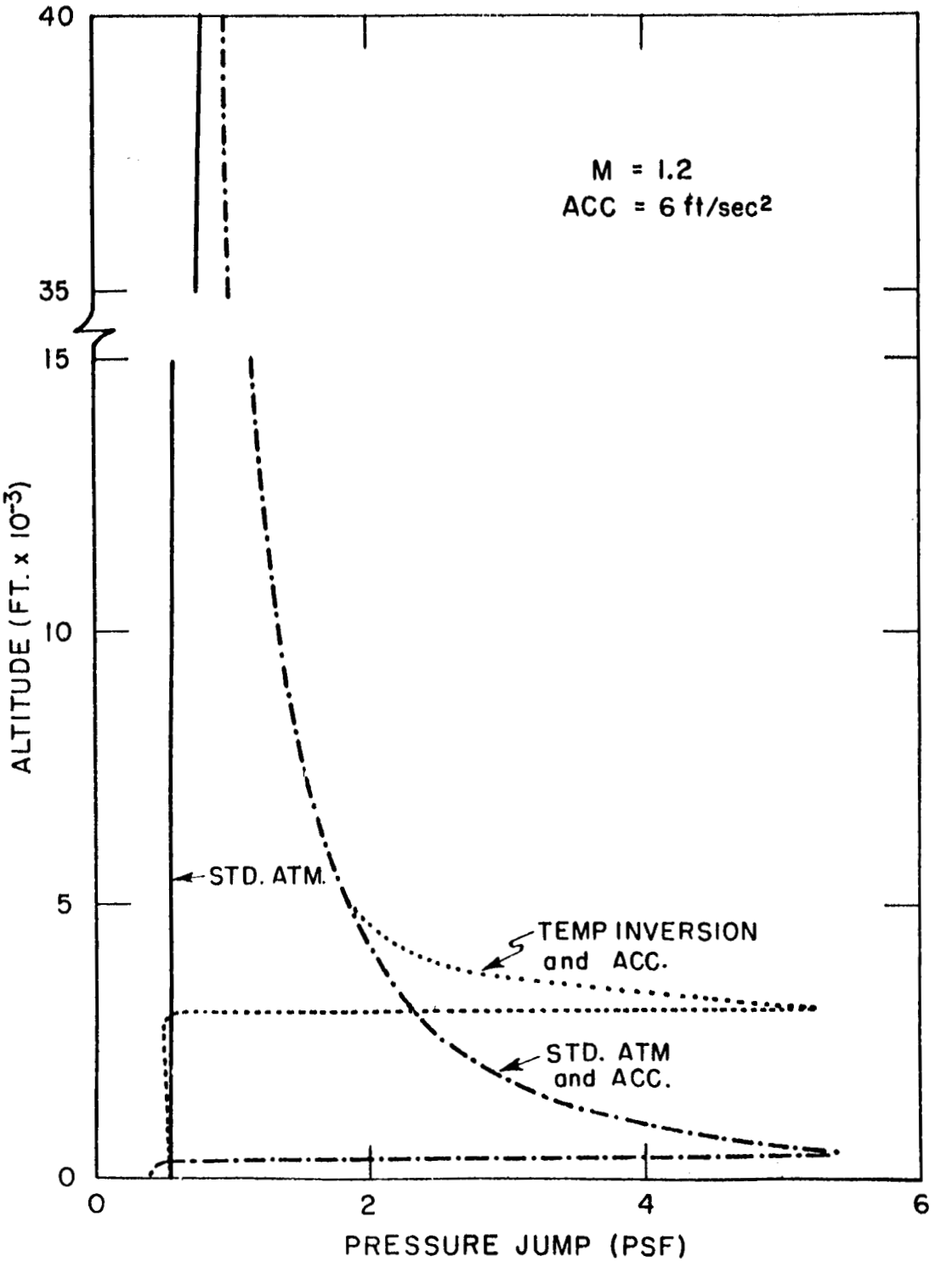

Figure AV.4. Aircraft accel. and temp. inversion, alt. = 56,000 ft.

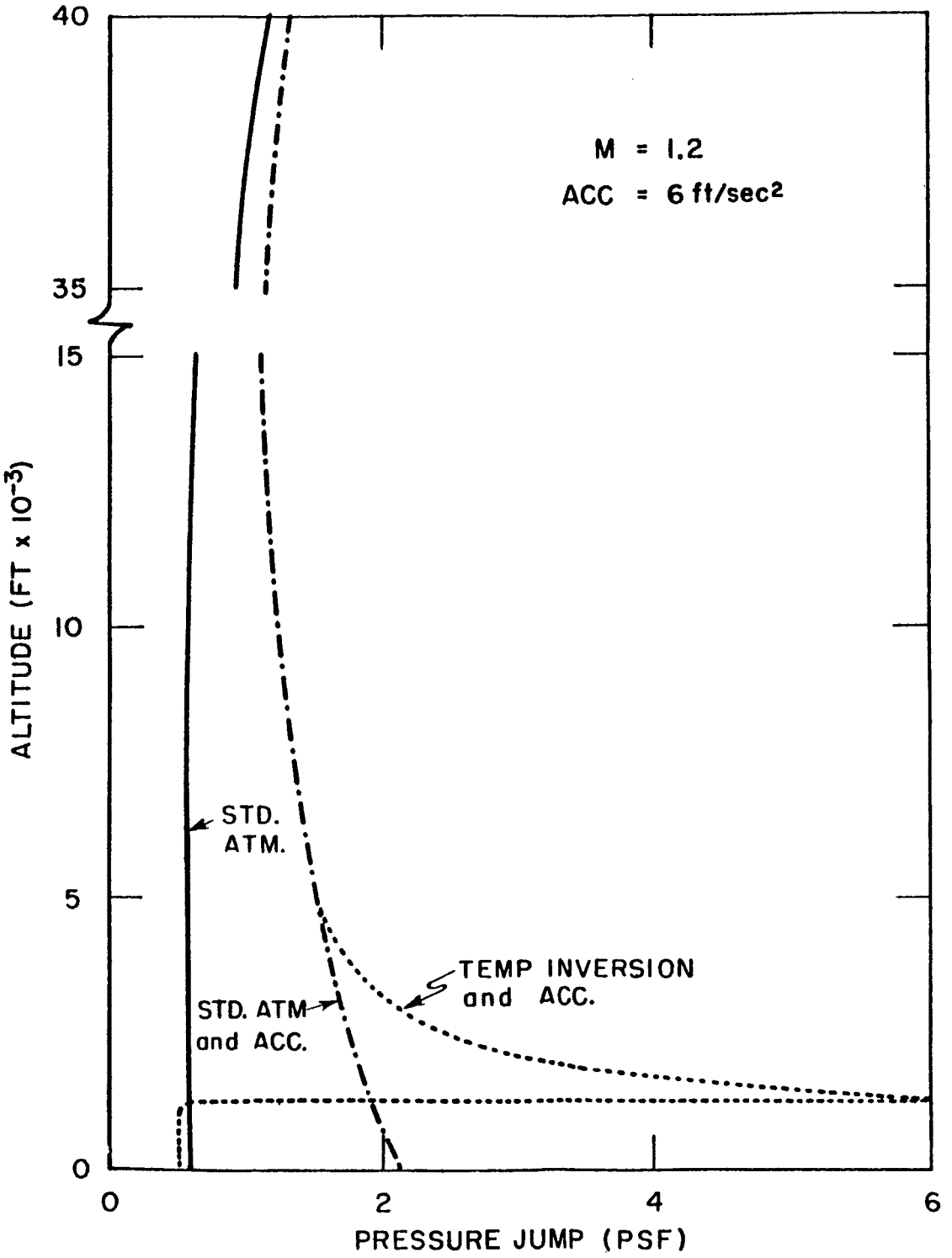

Figure AV.5. Aircraft accel. and temp. inversion, alt. = 50,000 ft.

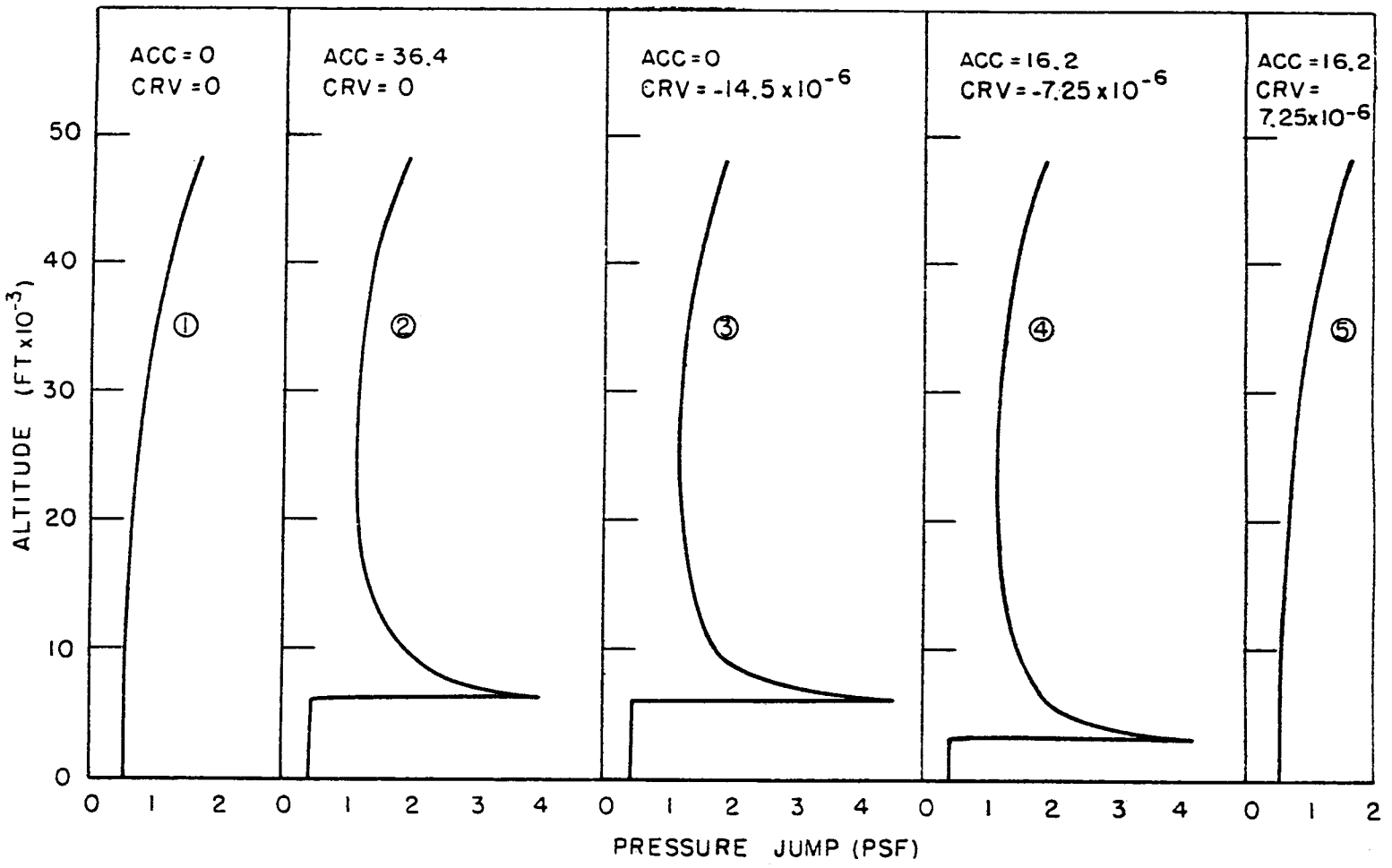

Figure AV.6. Aircraft acceleration and flight path curvature, dive angle = 15°, M = 1.5, alt. = 60,000 ft.

SONIC BOOM, CASE 0, M= 1.500, ALTITUDE= 60000., ACC= 0. , RC=1.80, VF= 0.640, LF= 0.
WT= 100000.0, LENGTH= 100.0, FR= 8.00, WL=50.000, PSI= -15.00, TAU= 5.00SEC., CURVATURE= 0.

ALTITUDE (FT)	HEADWIND (FPS)	SIDEWIND (FPS)	PRESSURE (PSF)	SOUND SPEED (FPS)	TEMPERATURE (DEG F)
60000.	-0.	-0.	657.600	998.446	-44.400
8000.	-0.	-0.	657.600	998.446	-44.400
0.	-0.	-0.	657.600	998.446	-44.400

HISTORY OF SHOCK STRENGTH VARIATION, ANGLE= 0.

Z (FT)	X (FT)	Y (FT)	PRESSURE RATIO	PRESSURE JUMP (PSF)	PRESSURE (PSF)
48000.	-6065.	-0.	0.0025819	1.698	657.600
46000.	-7077.	-0.	0.0023288	1.531	657.600
44000.	-8089.	-0.	0.0021082	1.386	657.600
42000.	-9101.	-0.	0.0019286	1.268	657.600
40000.	-10113.	-0.	0.0017807	1.171	657.600
38000.	-11125.	-0.	0.0016569	1.090	657.600
36000.	-12137.	-0.	0.0015590	1.025	657.600
34000.	-13148.	-0.	0.0014614	0.961	657.600
32000.	-14160.	-0.	0.0013870	0.912	657.600
30000.	-15171.	-0.	0.0013175	0.866	657.600
28000.	-16183.	-0.	0.0012548	0.825	657.600
26000.	-17194.	-0.	0.0011985	0.788	657.600
24000.	-18206.	-0.	0.0011476	0.755	657.600
22000.	-19217.	-0.	0.0011016	0.724	657.600
20000.	-20228.	-0.	0.0010596	0.697	657.600
18000.	-21240.	-0.	0.0010212	0.672	657.600
16000.	-22251.	-0.	0.0009859	0.648	657.600
14000.	-23262.	-0.	0.0009533	0.627	657.600
12000.	-24273.	-0.	0.0009231	0.607	657.600
10000.	-25285.	-0.	0.0008950	0.589	657.600
8000.	-26296.	-0.	0.0008689	0.571	657.600
6000.	-27307.	-0.	0.0008486	0.558	657.600
4000.	-28318.	-0.	0.0008276	0.541	657.600
2000.	-29329.	-0.	0.0008043	0.529	657.600
0.	-30341.	-0.	0.0007810	0.514	657.600

SONIC BOOM, CASE 0, M= 1.500

ANGLE (DEG)	PRESSURE JUMP (PSF)	X (FT)	Y (FT)	TIME (SEC)
RAY-GROUND DATA				
ALTITUDE = 60000.				
-30.00	0.850	-35971.	28111.	75.47
0.	0.924	-30341.	-0.	67.31
15.00	0.904	-31654.	-13344.	69.21
30.00	0.850	-35971.	-28111.	75.47
ALTITUDE = 58062.				
-30.00	0.873	-42043.	27203.	78.04
0.	0.947	-36594.	-0.	70.13
15.00	0.928	-37865.	-12913.	71.98
30.00	0.873	-42043.	-27203.	78.04
SHOCK-GROUND DATA				
-30.00	0.829	-30595.	28915.	73.21
0.	0.971	-43396.	0.	73.21
15.00	0.939	-40629.	-12721.	73.21
30.00	0.829	-30595.	-28915.	73.21